Benchmarking Nitrous Oxide Adsorption and Activation in Metal-Organic Frameworks Bearing Coordinatively Unsaturated Metal Centers

Tristan A. Pitt,[a] Haojun Jia,[b,c] Tyler J. Azbell,[a] Mary E. Zick,[a] Aditya Nandy,[b,c] Heather J. Kulik,[b,c] Phillip J. Milner[a,*]

[a]Department of Chemistry and Chemical Biology, Cornell University, Ithaca, NY, 14850, United States
[b]Department of Chemical Engineering, Massachusetts Institute of Technology, Cambridge, MA, 02139, United States
[c]Department of Chemistry, Massachusetts Institute of Technology, Cambridge, MA, 02139, United States

*pjm347@cornell.edu

Supporting Information

Table of Contents

1. General procedures

All reagents were purchased from commercial vendors and used without further purification unless specified otherwise. The solvents ethanol (EtOH, Fisher, ACS Grade), diethyl ether (Et_2O, Fischer, 99%), glacial acetic acid (HOAc, Fisher, ACS Grade), methanol (MeOH, Fisher, ACS Grade), *N*,*N*-dimethylformamide (DMF, Fisher, ACS Grade), and isopropanol (*i*PrOH, Fisher, ACS Grade) were purchased from commercial vendors. Dry, degassed solvents were obtained in SureSeal bottles and stored over 3 Å sieves or were obtained by sparging with Ar for 30 min and then passing the solvent through two columns of activated alumina using a JC Meyer solvent system. All dry, degassed solvents were stored over 3 Å sieves in an N_2-filled glovebox when not in use. The reagents trifluoroacetic anhydride (TFAA, AESAR, 99%), fuming nitric acid (HNO_3, VWR, ACS Grade), dibenzo-1,4-dioxin, 37% hydrochloric acid (conc. HCl, J.T. Baker, ACS Grade), tin powder (AESAR, 99.5%), sodium nitrite ($NaNO_2$, AESAR, ACS Grade), 2,5-dihydroxyterephthalic acid (H_4dobdc, Astatech, 95%), $Mg(NO_3)_2{\cdot}6H_2O$ (Beantown, 98%), $MnCl_2{\cdot}4H_2O$ (Fisher, 98%), anhydrous $FeCl_2$ (AESAR, 98%), $Co(NO_3)_2{\cdot}6H_2O$ (Aldrich, 98%), $Ni(NO_3)_2{\cdot}6H_2O$ (Acros, 98%), $Cu(NO_3)_2{\cdot}6H_2O$, $Zn(NO_3)_2{\cdot}6H_2O$ (Lancaster, 99%), $CoCl_2{\bullet}6H_2O$ (Aldon, Reagent Grade), $NiCl_2{\bullet}6H_2O$ (Acros, 99.95%), and $CuCl_2{\cdot}2H_2O$ (Aldrich, ACS Grade) were purchased from commercial vendors. Deuterated dimethyl sulfoxide (DMSO-d_6, 99%) was purchased from Cambridge Isotope Laboratories. Cylinders of N_2 (Ultra High Purity, 99.999%) and N_2O (UHP 4, 99.99%) were purchased from Airgas.

Powder X-ray diffraction (PXRD) patterns were collected on a Rigaku Ultima IV diffractometer equipped with a Cu K_α source (λ = 1.54 Å) and were baseline-corrected using OriginPro. Diffraction data on air-sensitive samples were collected by packing a small amount of material (5–10 mg) into a glass capillary (1.0 mm outer diameter, Charles Supper) in a N_2-filled glovebox and sealed under N_2 using a large plug of silicon grease. The effect of the sample preparation on the peak profiles and 2θ positions of sample reflections relative to a uniform flattened powder sample was modeled using Mg_2(dobdc) (Figure S1) and on that basis a value of 0.22 ° 2θ was uniformly subtracted from the data collected in capillaries to account for the artificial shift to higher angles caused by the sample preparation. NMR data were collected on a Bruker INOVA 500 MHz spectrometer and are referenced to residual solvent. Infrared (IR) spectra were collected on a Bruker Tensor II IR spectrometer equipped with a diamond Attenuated Total Reflectance (ATR) attachment. Variable temperature diffuse reflectance infrared Fourier transform spectroscopy (DRIFTS) spectra were collected on a Bruker Tensor II IR spectrometer with a Harrick Praying Mantis attachment. Magnetic susceptibility measurements were performed using a Quantum Design MPMS3 superconducting quantum interference device (SQUID) magnetometer under an applied magnetic field of 1000 Oe. Moment vs. field measurements were performed using a Quantum Design Dynacool Physical Property Measurement System (PPMS) at 5 K and the field was swept from –9 T to 9 T at a rate of 200 Oe per second. In all cases, powder samples were loaded into plastic sample holders in a N_2-filled glovebox.

Surface area data were collected on a Micromeritics ASAP 2020 gas sorption analyzer using Ultra High Purity N_2 (99.999%) and a liquid N_2 bath. N_2O adsorption data were fit using the dual-

site Langmuir-Freundlich model (eq. S1), where $Q(P)$ is the predicted uptake Q at pressure P in mmol/g, $Q_{sat,i}$ is the saturation pressure of binding site i in mmol/g, b_i is the Langmuir parameter of site i, v_i is the Freundlich parameter of site i, $-S_i$ is the entropy of binding site i in J/mol•K, R is the ideal gas constant, E_i is the enthalpy of adsorption for binding site i in kJ/mol, and T is the temperature in K. The isotherms were fit with v_1 and v_2 allowed to vary freely (dual-site Langmuir-Freundlich model). Fits were obtained using Solver in Microsoft Excel.

$$Q(P) = \frac{Q_{sat1}(b_1P)^{v_1}}{1+(b_1P)^{v_1}} + \frac{Q_{sat2}(b_2P)^{v_2}}{1+(b_2P)^{v_2}}; b_i = e^{\left(\frac{-S_i}{R}\right)\left(\frac{1000 \cdot E_i}{RT}\right)} \quad \text{eq. S1}$$

Heats of adsorption ($-\Delta H_{ads}$) values were calculated using the Clausius-Clapeyron equation (eq. S2), where P_Q are pressure values corresponding to the same loading Q, ΔH_{ads} is the differential enthalpy of adsorption in kJ/mol, R is the ideal gas constant, T is the temperature in K, and c is a constant. Fits over a range of Q values were obtained using Mathematica to calculate the differential enthalpies of adsorption (ΔH_{ads}) based on the slopes of the linear trendlines fit to $\ln(P_Q)$ vs 1/T at constant values of Q.

$$\ln(P_Q) = \left(\frac{\Delta H_{ads}}{R}\right)\left(\frac{1}{T}\right) + c \quad \text{eq. S2}$$

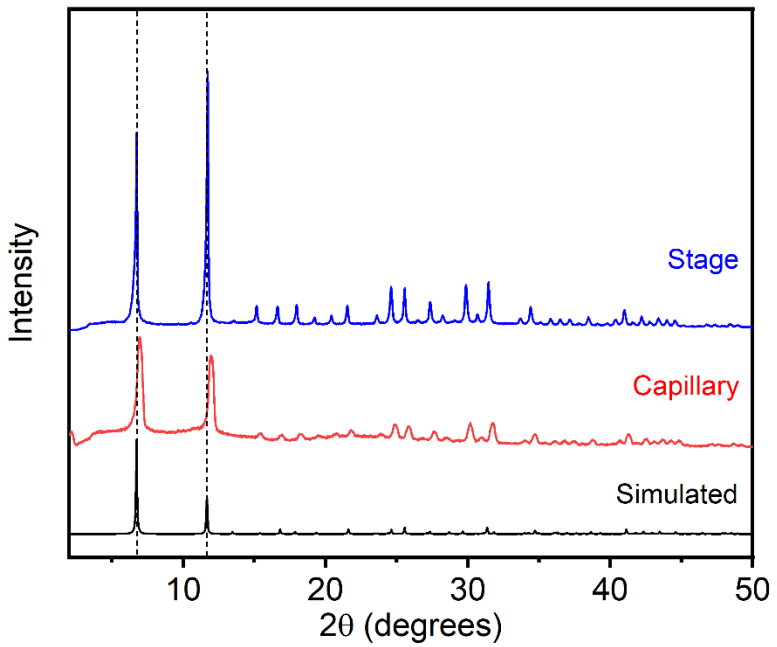

Figure S1. PXRD (λ = 1.54 Å) patterns of identical Mg_2(dobdc) samples prepared in a capillary (red) or as a uniform flattened layer (blue). The simulated pattern (black) based on the single-crystal X-ray diffraction (SCXRD) structure of the isostructural MOF Zn_2(dobdc) is included for reference.[1]

2. Synthesis and characterization of H_2btdd.

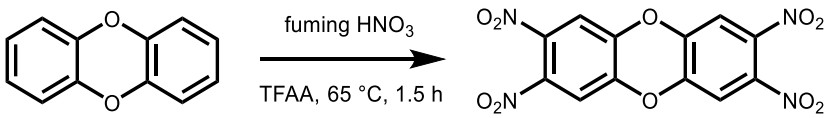

This procedure is adapted from the literature.[2] A 50 mL round bottom flask equipped with a stir bar and reflux condenser was cooled to 0 °C using an ice water bath. Trifluoroacetic anhydride (3.6 mL) was added slowly at 0 °C, followed by fuming nitric acid (4.5 mL). Next, dibenzo-1,4-dioxin (1.09 g, 5.92 mmol, 1.00 equiv.) was added in portions over 10 min with vigorous stirring. The reaction mixture was allowed to warm to room temperature and then stirred at 65 °C for 1.5 h. The reaction mixture was allowed to cool to room temperature and then poured into cold H_2O (100 mL). The heterogeneous mixture was filtered, and the resulting solid was rinsed with H_2O (100 mL). Drying under vacuum for 12 h yielded 2,3,7,8-tetranitrodibenzo-1,4-dioxin (1.83 g, 85%) as a bright yellow solid. ^{1}H NMR (500 MHz, DMSO-d_6): δ 8.03 (s, 4H) ppm. This spectrum is consistent with that reported in the literature.[2]

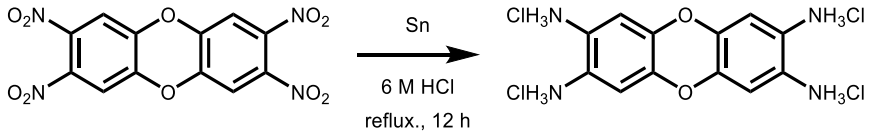

This procedure is adapted from the literature.[3] A 250 mL round bottom flask equipped with a stir bar and reflux condenser was charged with 2,3,7,8-tetranitrodibenzo-1,4-dioxin (1.83 g, 5.02 mmol, 1.00 equiv.) and 6 M HCl (44 mL). Sn powder (7.52 g, 63.7 mmol, 12.7 equiv.) was added in portions over 10 min with vigorous stirring. The reaction mixture was stirred for 30 min at room temperature and then heated to reflux for 12 h with stirring. The reaction mixture was allowed to cool to room temperature and filtered. The resulting solid was rinsed with 6 M HCl (100 mL), EtOH (100 mL), and Et_2O (100 mL). Drying under vacuum for 12 h yielded dibenzo-1,4-dioxin-2,3,7,8-tetraamine hydrochloride (3.91 g, 78%) as a green solid. ^{1}H NMR (500 MHz, DMSO-d_6): δ 6.61 (bs, 4H) ppm. This spectrum is consistent with that reported in the literature.[3]

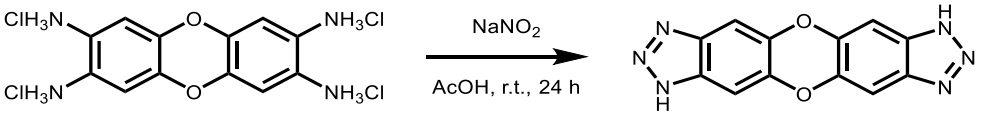

This procedure is adapted from the literature.[2] A 100 mL round bottom flask equipped with a stir bar was charged with dibenzo-1,4-dioxin-2,3,7,8-tetraamine hydrochloride (1.53 g, 6.25 mmol, 1.00 equiv.), glacial AcOH (15 mL), and H_2O (2 mL). The flask was cooled to 0 °C using an ice water bath. Separately, $NaNO_2$ (0.65 g, 9.38 mmol, 1.50 equiv.) was dissolved in H_2O (3 mL). The $NaNO_2$ solution was added dropwise to the substrate solution at 0 °C. The reaction mixture was allowed to warm to room temperature and stirred for 24 h at room temperature. H_2O (100 mL) was

added, and the heterogeneous reaction mixture was filtered. The resulting brown solid was rinsed with H_2O (100 mL) and MeOH (100 mL). Drying under vacuum for 12 h yielded bis(1*H*-1,2,3-triazolo[4,5-b],[4',5'-i])dibenzo[1,4]dioxin) (H_2btdd, 1.31 g, 79%) as a brown solid. ^{1}H NMR (500 MHz, DMSO-d6): δ 15.6 (bs, 2H), 7.63 (bs, 4H) ppm. This spectrum is consistent with that reported in the literature.[2]

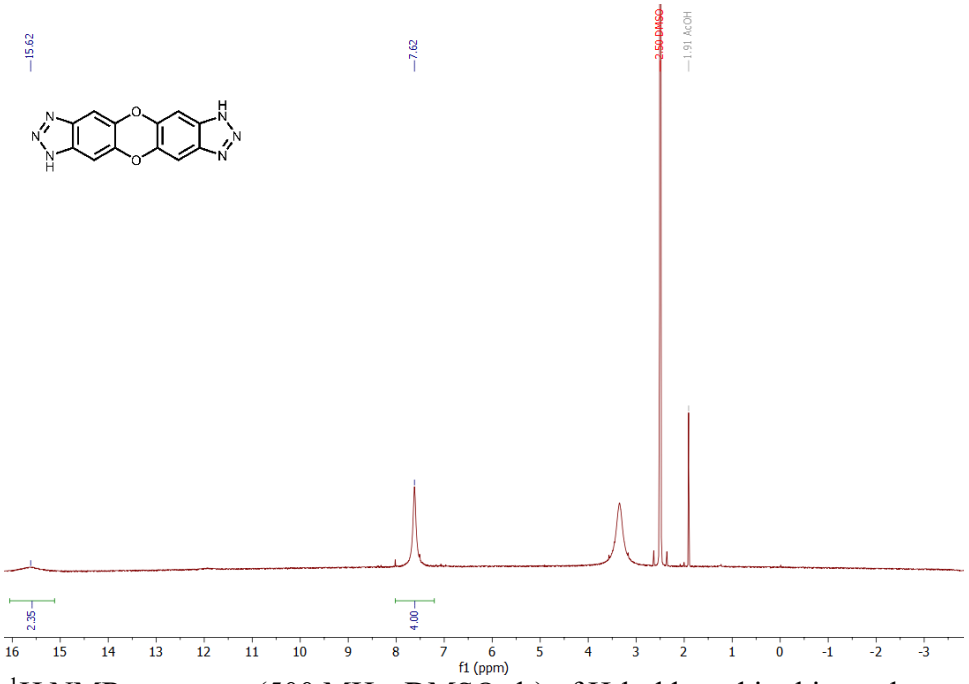

Figure S2. ^{1}H NMR spectrum (500 MHz, DMSO-d_6) of H_2btdd used in this work.

3. Synthesis, characterization, and gas sorption analysis of $Mn_2Cl_2(btdd)$.

Synthesis of $Mn_2Cl_2(btdd)$. This procedure is adapted from the literature.[4] A 500 mL round-bottom flask was charged with H_2btdd (0.200 g, 0.75 mmol, 1.00 equiv.) and DMF (200 mL). The mixture was heated to 130 °C with stirring until the linker dissolved, and then the solution was allowed to cool to room temperature. Separately, $MnCl_2•4H_2O$ (0.296 g, 1.50 mmol, 2.00 equiv.) was dissolved in EtOH (200 mL) and concentrated HCl (4 mL) in a 500 mL Pyrex jar. Once cooled, the H_2btdd solution was added to the $MnCl_2•4H_2O$ solution and the jar was capped. The jar was placed in an oven that had been pre-heated to 60 °C and allowed to stand at 60 °C for 10 d. After this time, the jar was removed from the oven, and the heterogeneous reaction mixture was filtered. The collected solids were returned to the jar and suspended in fresh DMF (100 mL). The jar was returned to the oven and allowed to stand for 24 h at 60 °C, at which time the heterogenous mixture was filtered, and the collected solids were returned to the jar and suspended in fresh DMF (100 mL). This procedure was repeated two additional times for a total of three hot DMF soaks. Next, the mixture was filtered and the collected solid was returned to the jar and suspended in fresh MeOH (100 mL). The solid was soaked in MeOH for 24 h at 60 °C in an oven three total times following the same procedure as described above. The heterogeneous mixture was filtered and the collected solid was transferred to a Schlenk flask. The material was activated under high vacuum (<100 mbar) at 100 °C for 24 h, and the Schlenk flask was transferred into a N_2-filled glovebox. Activated $Mn_2Cl_2(btdd)$ was obtained as an off-white solid. Prior to gas sorption analysis, the material was activated for an additional 24 h under high vacuum (<10 μbar) at 180 °C.

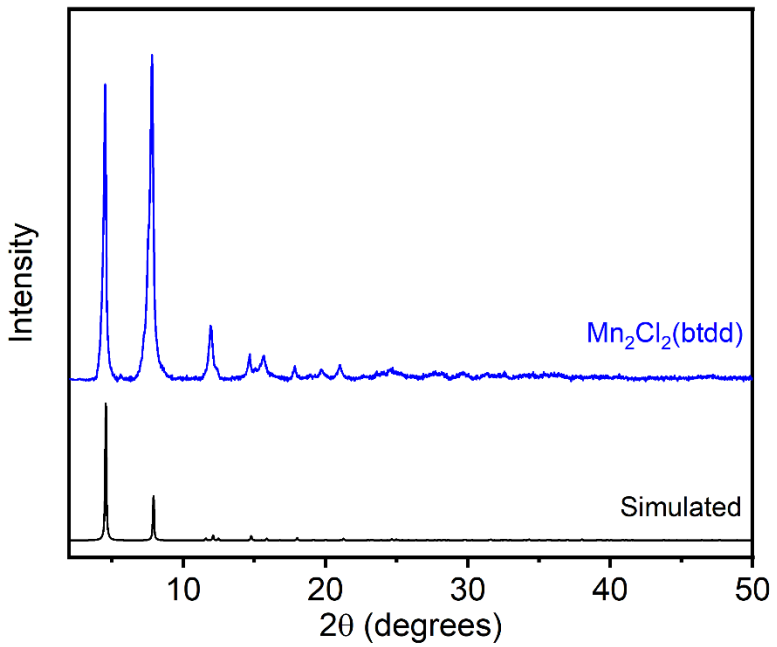

Figure S3. PXRD (λ = 1.54 Å) pattern of MeOH-solvated $Mn_2Cl_2(btdd)$. The simulated pattern (black) based on the SCXRD structure of $Mn_2Cl_2(btdd)$ is included for reference.[4]

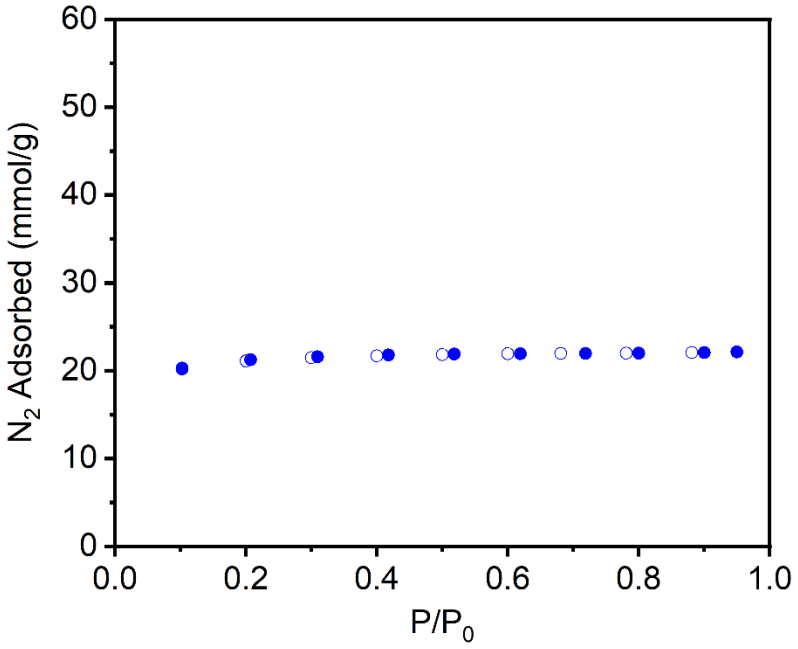

Figure S4. N_2 adsorption (solid circles) and desorption (open circles) isotherms of activated Mn_2Cl_2(btdd) at 77 K. The Langmuir surface area of this material was determined to be 2169 ± 3 m^2/g (Literature BET: 1917 m^2/g).[4] The unusually low surface area of this material compared to the other M_2Cl_2(btdd) MOFs studied herein is likely due to its air sensitivity.

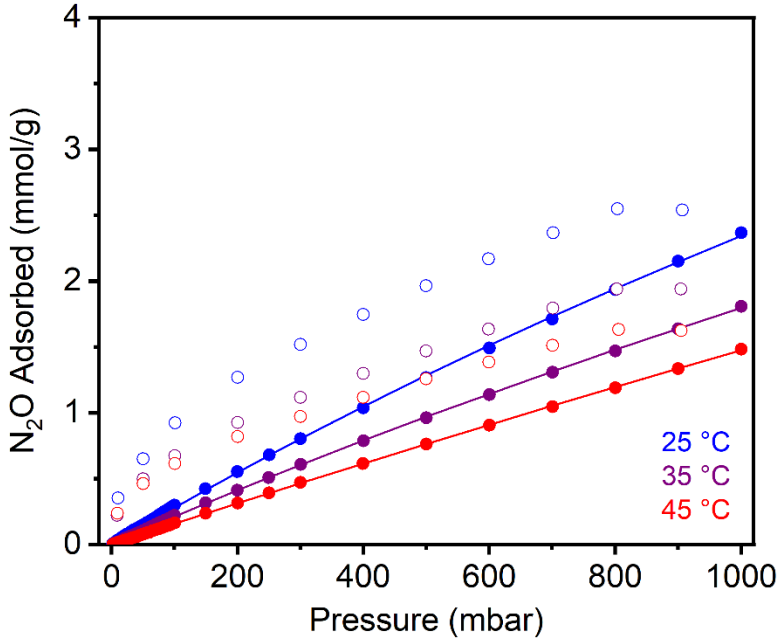

Figure S5. N_2O adsorption (solid circles) and desorption (open circles) isotherms of activated Mn_2Cl_2(btdd) at 25 °C (blue), 35 °C (purple), and 45 °C (red). Solid lines represent fits to the dual-site Langmuir-Freundlich model. The sample was reactivated at 180 ºC for 24 h under high vacuum (<10 μbar) between isotherms. A data point was considered equilibrated when less than 0.01% change in pressure occurred over a 30 or 60 s interval.

Table S1. Langmuir-Freundlich fit parameters determined from the fits in Figure S5.

	25 °C	35 °C	45 °C
$Q_{sat}1$ (mmol/g)	13.2	20.7	29.0
S1 (in multiples of R)	4.94	7.69	7.77
E1 (kJ/mol)	8.46	13.3	12.4
V1	1.00	1.00	1.00
$Q_{sat}2$ (mmol/g)	0.00	0.513	1.09
S2 (in multiples of R)	0.029	0.041	1.38
E2 (kJ/mol)	0.030	0.00	0.00
V2	1.00	1.00	1.00

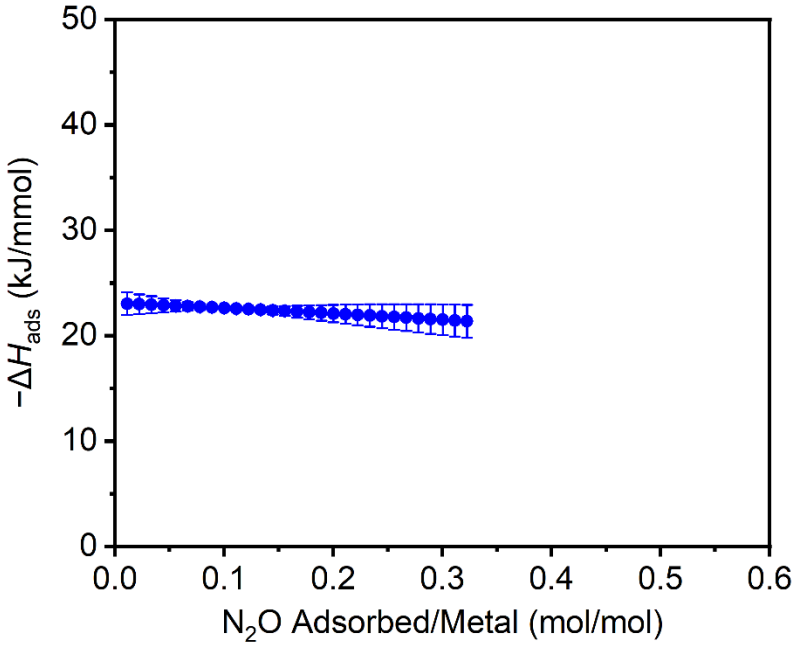

Figure S6. $-\Delta H_{ads}$ for N_2O adsorption as a function of uptake per open metal site in Mn_2Cl_2(btdd), as determined using the fits in Figure S5.

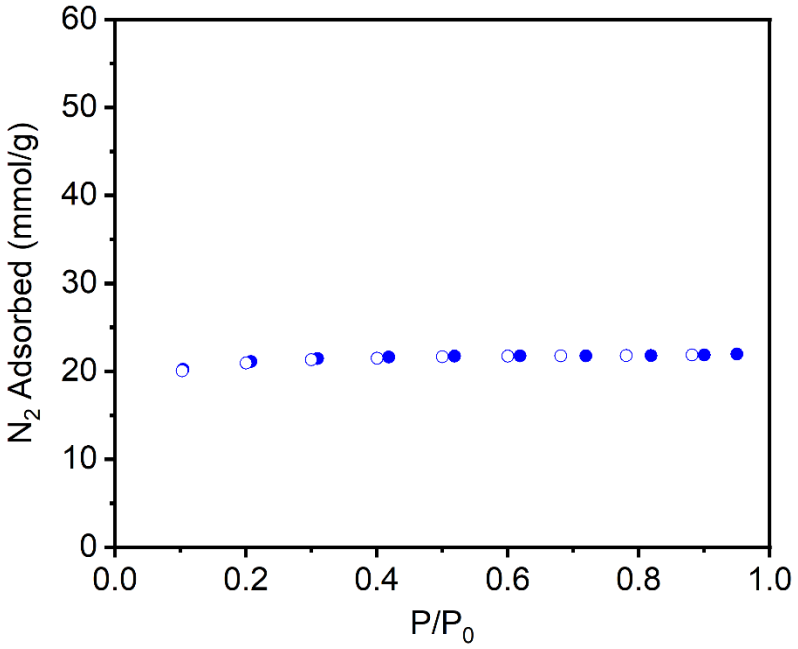

Figure S7. N_2 adsorption (solid circles) and desorption (open circles) isotherms of activated $Mn_2Cl_2(btdd)$ at 77 K after the N_2O adsorption isotherms. The Langmuir surface area of this material was determined to be 2149 ± 4 m^2/g.

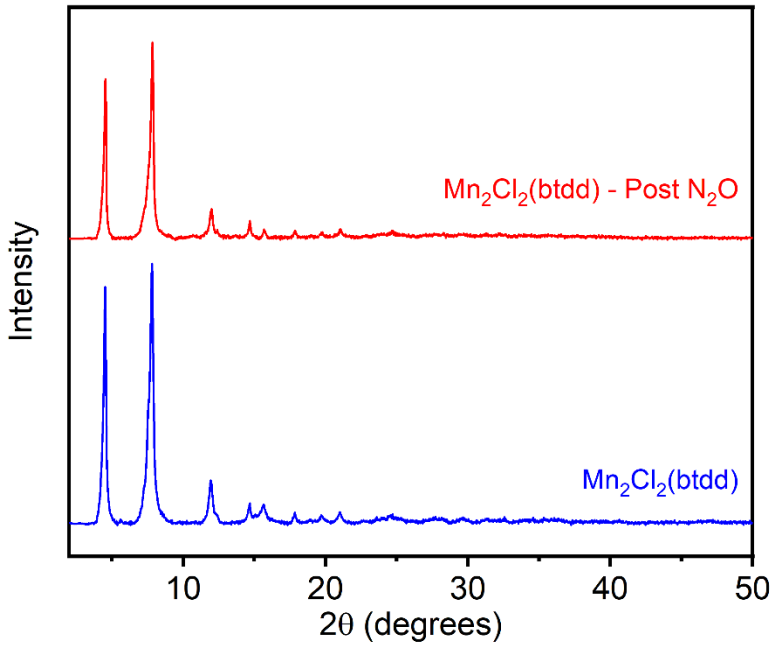

Figure S8. PXRD (λ = 1.54 Å) pattern of activated $Mn_2Cl_2(btdd)$ after the N_2O adsorption isotherms. The experimental pattern prior to the N_2O adsorption isotherms is included for reference.

4. Synthesis, characterization, and gas sorption analysis of Co_2Cl_2(btdd).

Synthesis of Co_2Cl_2(btdd). This procedure is adapted from the literature.[4] A 1 L round-bottom flask was charged with H_2btdd (0.400 g, 1.50 mmol, 1.00 equiv.) and DMF (400 mL). The mixture was heated to 120 °C with stirring until the linker dissolved, and then the solution was allowed to cool to room temperature. Separately, $CoCl_2$•$6H_2O$ (0.714 g, 3.00 mmol, 2.00 equiv.) was dissolved in EtOH (400 mL) and concentrated HCl (8 mL) in a 1 L Pyrex jar. Once cooled, the H_2btdd solution was then added to the $CoCl_2$•$6H_2O$ solution and the jar was capped. The jar was placed in an oven that had been pre-heated to 60 °C and allowed to stand at 60 °C for 10 d. After this time, the jar was removed from the oven, and the heterogeneous reaction mixture was filtered. The collected solids were returned to the jar and suspended in fresh DMF (500 mL). The jar was returned to the oven and allowed to stand for 24 h at 60 °C, after which time the heterogenous mixture was filtered and the collected solids were returned to the jar and suspended in fresh DMF (500 mL). This procedure was repeated two additional times for a total of three hot DMF soaks. Next, the mixture was filtered, and the collected solid was returned to the jar and suspended in fresh MeOH (500 mL). The solid was soaked in MeOH for 24 h at 60 °C in an oven three total times following the same procedure as described above. The heterogeneous mixture was filtered and the collected solid was transferred to a Schlenk flask. The material was activated under high vacuum (<100 mbar) at 100 °C for 24 h, then the Schlenk flask was transferred into a N_2-filled glovebox. Activated Co_2Cl_2(btdd) was obtained as a dark green solid. Prior to gas sorption analysis, the material was activated for an additional 24 h under high vacuum (<10 μbar) at 180 °C.

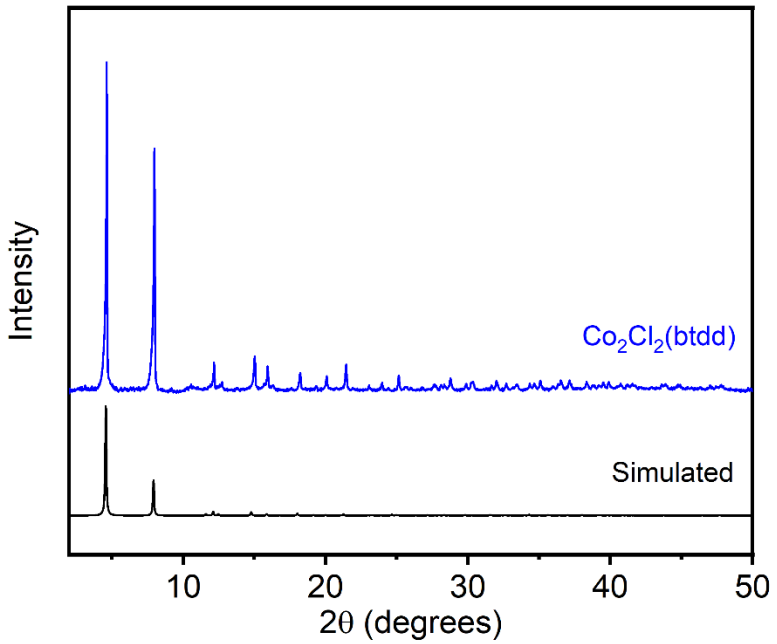

Figure S9. PXRD (λ = 1.54 Å) pattern of MeOH-solvated Co_2Cl_2(btdd). The simulated pattern (black) based on the SCXRD structure of the isostructural MOF Mn_2Cl_2(btdd) is included for reference.[4]

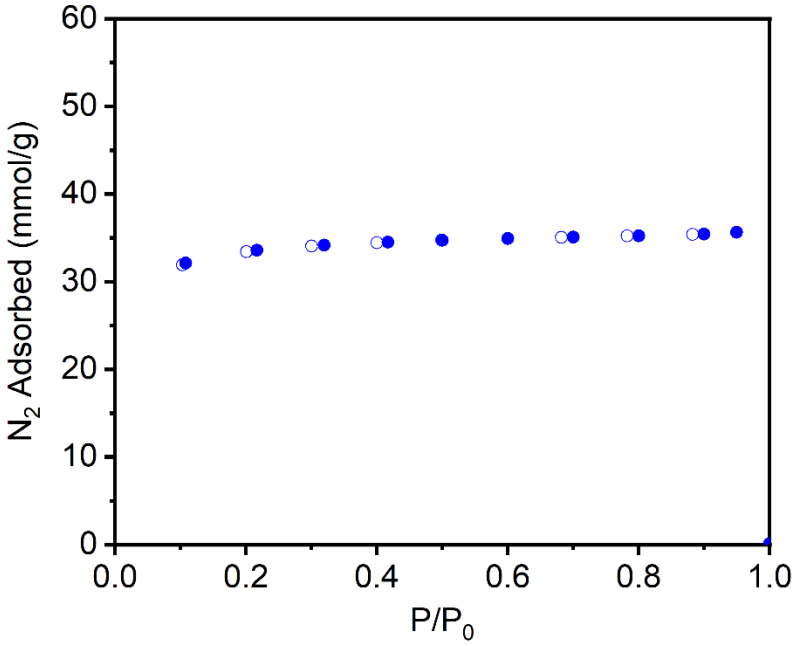

Figure S10. N_2 adsorption (solid circles) and desorption (open circles) isotherms of activated Co_2Cl_2(btdd) at 77 K. The Langmuir surface area of this material was determined to be 3500 ± 4 m^2/g (Literature BET: 1912 m^2/g).[4]

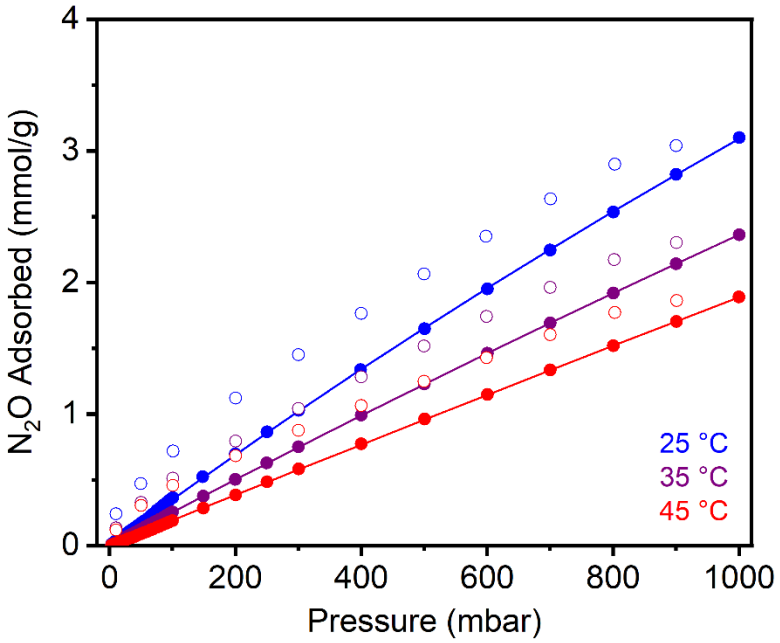

Figure S11. N_2O adsorption (solid circles) and desorption (open circles) isotherms of activated Co_2Cl_2(btdd) at 25 °C (blue), 35 °C (purple), and 45 °C (red). Solid lines represent fits to the dual-site Langmuir-Freundlich model. The sample was reactivated at 180 ºC for 24 h under high vacuum (<10 μbar) between isotherms. A data point was considered equilibrated when less than 0.01% change in pressure occurred over a 30 or 60 s interval.

Table S2. Langmuir-Freundlich fit parameters determined from the fits in Figure S11.

	25 °C	**35 °C**	**45 °C**
$Q_{sat}1$ (mmol/g)	23.7	31.5	73.1
S1 (in multiples of R)	3.91	3.95	4.74
E1 (kJ/mol)	4.99	3.69	2.94
V1	1.00	1.00	1.00
$Q_{sat}2$ (mmol/g)	0.00	0.00	0.00
S2 (in multiples of R)	0.016	0.012	0.031
E2 (kJ/mol)	0.030	0.00	0.00
V2	1.00	1.00	1.00

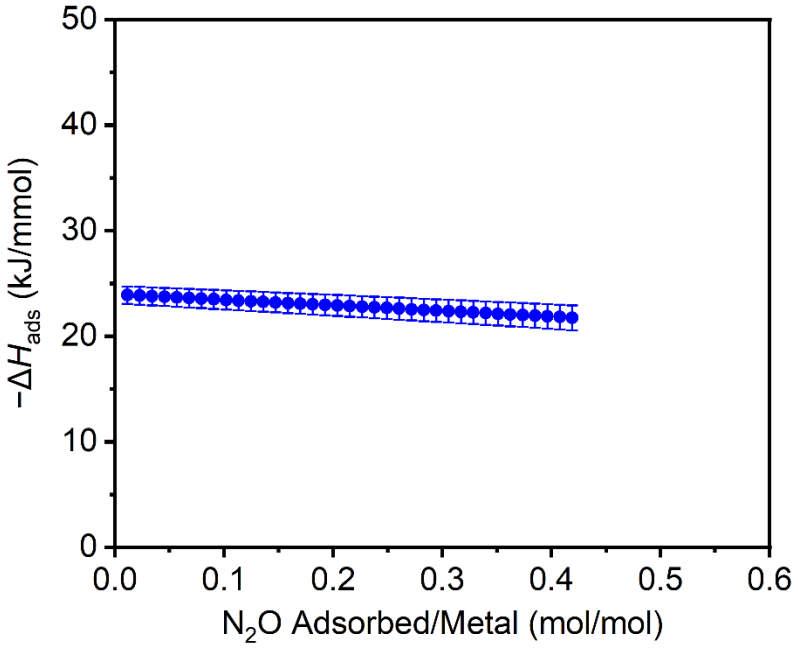

Figure S12. $-\Delta H_{ads}$ for N_2O adsorption as a function of uptake per open metal site in Co_2Cl_2(btdd), as determined using the fits in Figure S11.

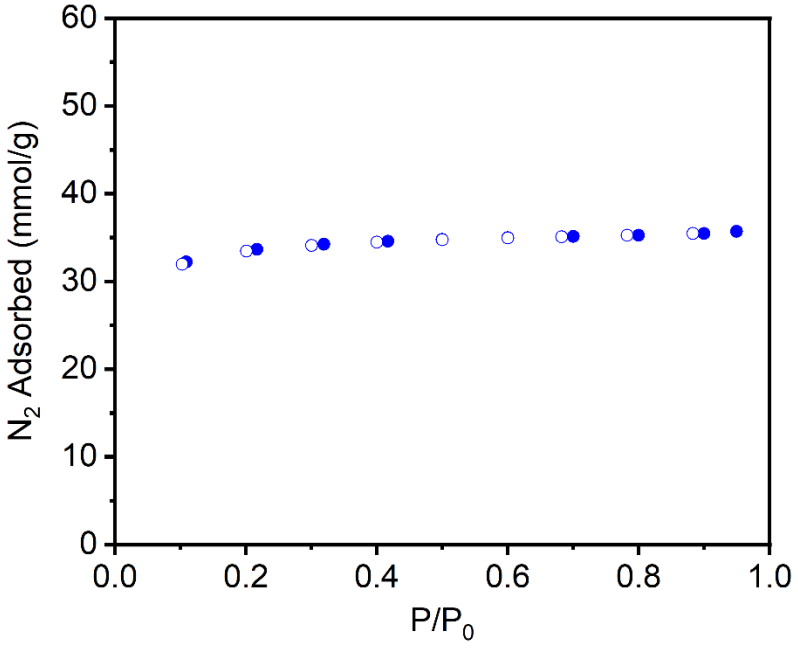

Figure S13. N_2 adsorption (solid circles) and desorption (open circles) isotherms of activated Co_2Cl_2(btdd) at 77 K after the N_2O adsorption isotherms. The Langmuir surface area of this material was determined to be 3505 ± 3 m^2/g.

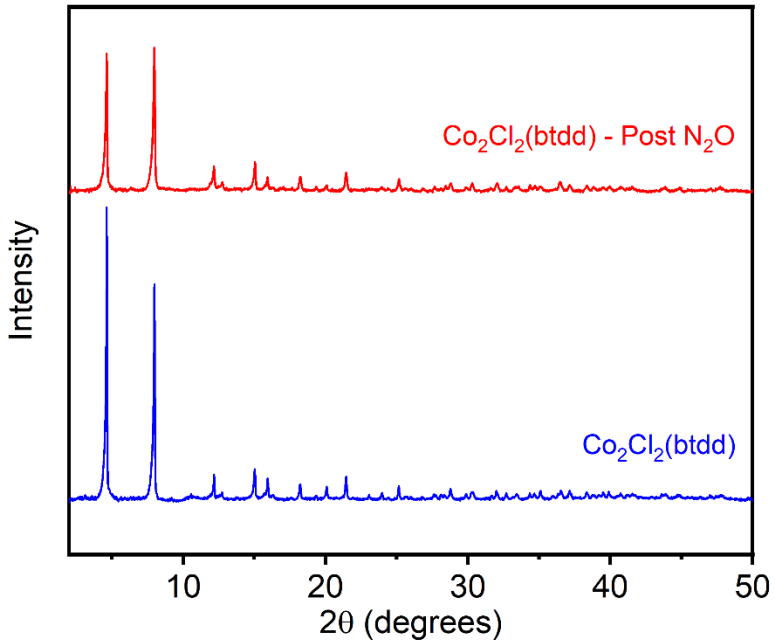

Figure S14. PXRD (λ = 1.54 Å) pattern of activated Co_2Cl_2(dobdc) after the N_2O adsorption isotherms. The experimental pattern prior to the N_2O adsorption isotherms is included for reference.

5. Synthesis, characterization, and gas sorption analysis of $Ni_2Cl_2(btdd)$.

Synthesis of $Ni_2Cl_2(btdd)$. This procedure is adapted from the literature.[5] Three 1 L Pyrex jars were each charged with H_2btdd (0.30 g, 1.13 mmol, 1.00 equiv.) and DMF (300 mL). The jars were sealed and placed in an oven that had been pre-heated to 100 °C. Once the linker dissolved, the jars were removed from the oven and allowed to cool to room temperature. Separately, three separate solutions of $NiCl_2$•$6H_2O$ (0.59 g, 2.48 mmol, 2.20 equiv.) dissolved in MeOH (300 mL) and concentrated HCl (192 mL) were prepared. The three $NiCl_2$•$6H_2O$ solutions were added separately to the three Pyrex jars containing the H_2btdd solutions. The jars were sealed and returned to the oven. The jars were allowed to stand at 100 °C for 2 d. At this time, the jars were removed from the oven, and the heterogeneous mixtures were filtered, combining the solids from all three jars into one sample. The collected solid was transferred to a 1 L Pyrex jar filled with fresh DMF (500 mL). The jar was allowed to stand for 24 h at room temperature, after which time the supernatant was decanted and replaced with fresh DMF (500 mL). This procedure was repeated two additional times for a total of three DMF soaks. Next, the mixture was filtered and the collected solid was returned to the jar and suspended in fresh MeOH (500 mL). The solid was soaked in MeOH for 24 h at room temperature in an oven three total times following the same procedure as described above. The heterogeneous mixture was filtered, and the collected solid was transferred to a Schlenk flask. The material was activated under flowing N_2 at 150 °C for 4 h, followed by further activation under high vacuum (<100 mbar) at 150 °C for 24 h. The Schlenk flask was transferred into a N_2-filled glovebox. Activated $Ni_2Cl_2(btdd)$ was obtained as a brown solid. Prior to gas sorption analysis, the material was activated for an additional 24 h under high vacuum (<10 μbar) at 180 °C.

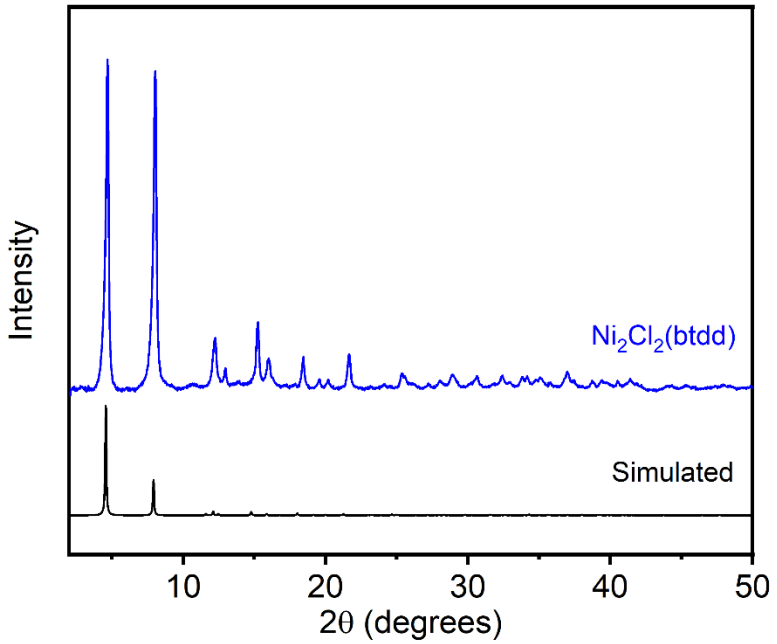

Figure S15. PXRD (λ = 1.54 Å) pattern of MeOH-solvated Ni_2Cl_2(btdd). The simulated pattern (black) based on the SCXRD structure of the isostructural MOF Mn_2Cl_2(btdd) is included for reference.[4]

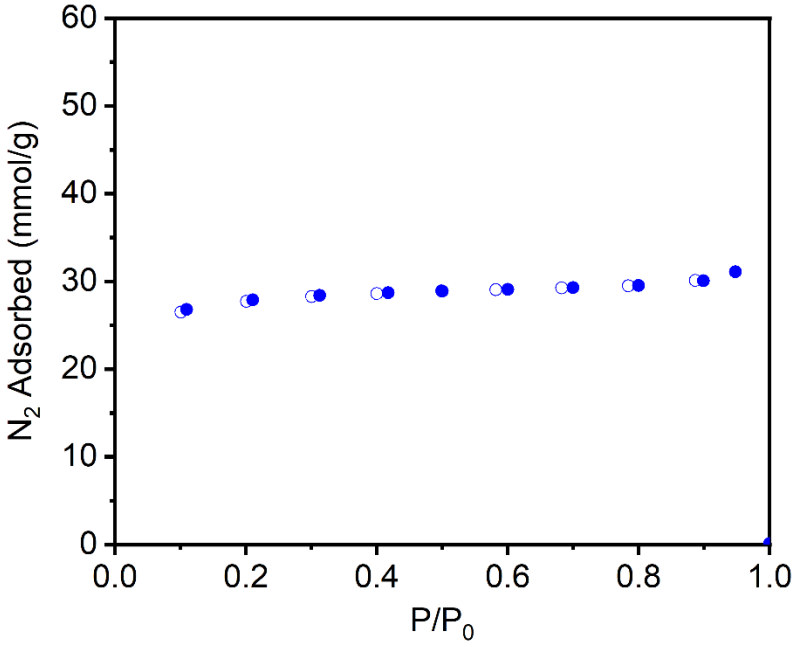

Figure S16. N_2 adsorption (solid circles) and desorption (open circles) isotherms of activated Ni_2Cl_2(btdd) at 77 K. The Langmuir surface area of this material was determined to be 2930 ± 9 m^2/g (Literature BET: 1837 m^2/g).[5]

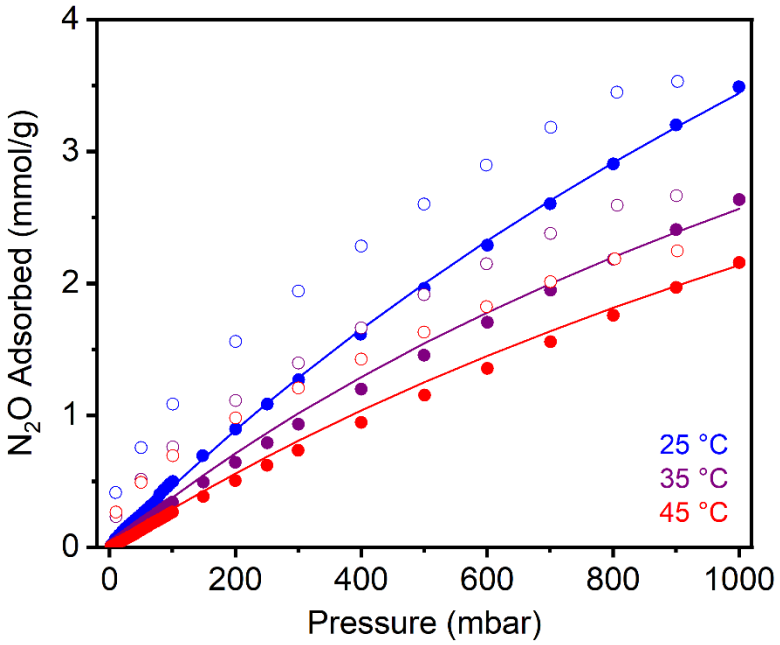

Figure S17. N_2O adsorption (solid circles) and desorption (open circles) isotherms of activated Ni_2Cl_2(btdd) at 25 °C (blue), 35 °C (purple), and 45 °C (red). Solid lines represent fits to the dual-site Langmuir-Freundlich model. The sample was reactivated at 180 ºC for 24 h under high vacuum (<10 μbar) between isotherms. A data point was considered equilibrated when less than 0.01% change in pressure occurred over a 30 or 60 s interval.

Table S3. Langmuir-Freundlich fit parameters determined from the fits in Figure S17.

	25 °C	**35 °C**	**45 °C**
$Q_{sat}1$ (mmol/g)	6.81	6.95	7.29
S1 (in multiples of R)	4.33	3.43	3.32
E1 (kJ/mol)	4.73	5.79	5.91
V1	1.00	1.00	1.00
$Q_{sat}2$ (mmol/g)	9.24	1.86	0.586
S2 (in multiples of R)	1.11	0.012	0.012
E2 (kJ/mol)	0.805	0.00	0.00
V2	1.00	1.00	1.00

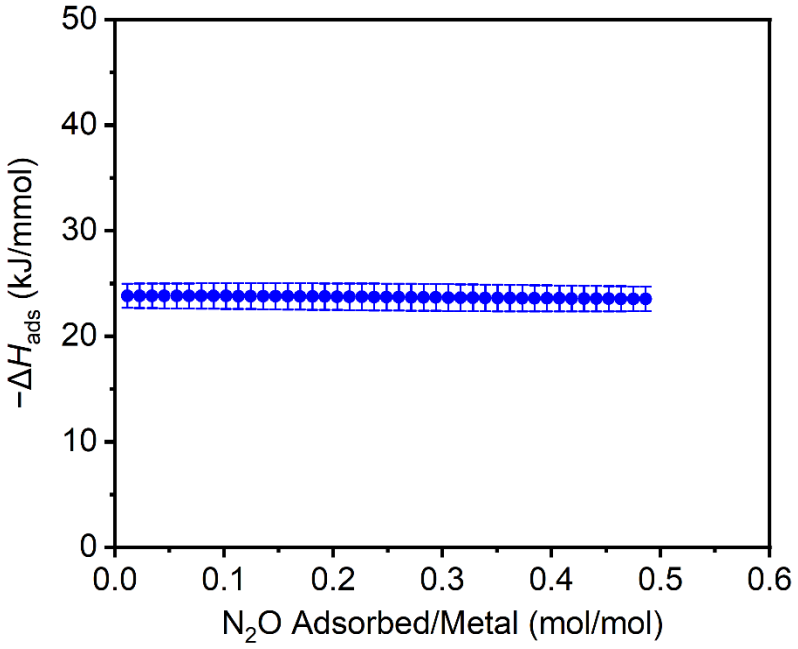

Figure S18. $-\Delta H_{ads}$ for N_2O adsorption as a function of uptake per open metal site in Ni_2Cl_2(btdd), as determined using the fits in Figure S17.

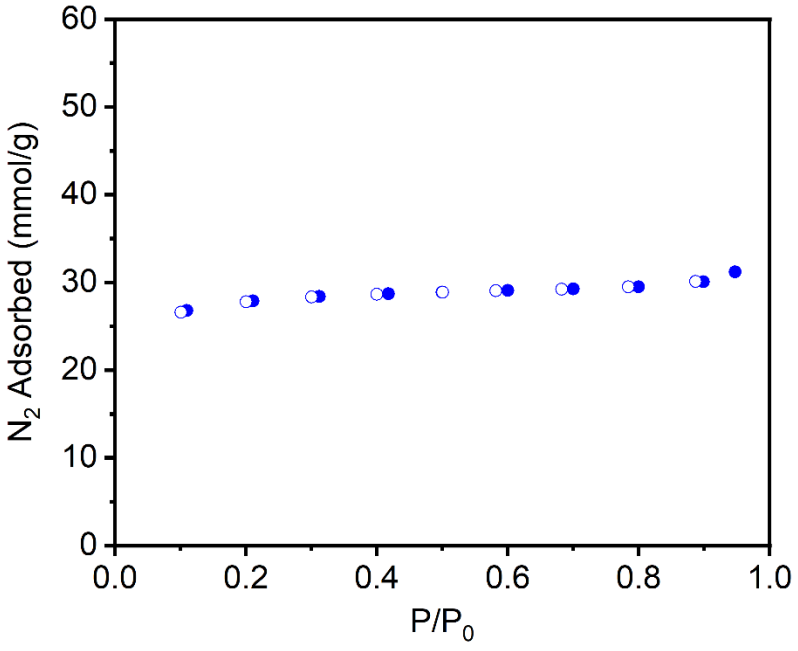

Figure S19. N_2 adsorption (solid circles) and desorption (open circles) isotherms of activated Ni_2Cl_2(btdd) at 77 K after the N_2O adsorption isotherms. The Langmuir surface area of this material was determined to be 2924 ± 7 m^2/g.

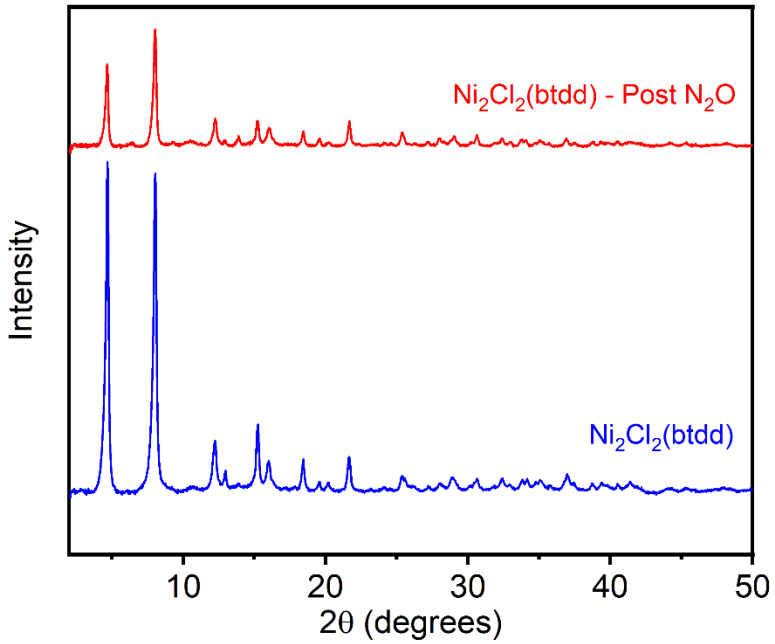

Figure S20. PXRD (λ = 1.54 Å) pattern of activated Ni_2Cl_2(btdd) after the N_2O adsorption isotherms. The experimental pattern prior to the N_2O adsorption isotherms is included for reference.

6. Synthesis, characterization, and gas sorption analysis of Cu_2Cl_2(btdd).

Synthesis of Cu_2Cl_2(btdd). This procedure is adapted from the literature.[6] A 1 L round-bottom flask was charged with H_2btdd (0.360 g, 1.35 mmol, 1.00 equiv.) and DMF (400 mL). The mixture was heated to 120 °C with stirring until the linker dissolved, and then the solution was allowed to cool to room temperature. Separately, $CuCl_2$•$2H_2O$ (0.464 g, 2.72 mmol, 2.02 equiv.) was dissolved in *i*PrOH (400 mL) and concentrated HCl (6.4 mL) in a 1 L Pyrex jar. Once cooled, the H_2btdd solution was added to the $CuCl_2$•$6H_2O$ solution and the jar was capped. The jar was placed in an oven that had been pre-heated to 60 °C and allowed to stand at 60 °C for 10 d. After this time, the jar was removed from the oven, and the heterogeneous reaction mixture was filtered. The collected solid was returned to the jar and suspended in fresh DMF (500 mL). The jar was returned to the oven and allowed to stand for 24 h at 60 °C, after which time the heterogenous mixture was filtered, and the collected solids were returned to the jar and suspended in fresh DMF (500 mL). This procedure was repeated two additional times for a total of three hot DMF soaks. Next, the mixture was filtered, and the collected solid was returned to the jar and suspended in fresh MeOH (500 mL). The solid was soaked in MeOH for 24 h at 60 °C in an oven three total times following the same procedure as described above. The heterogeneous mixture was filtered, and the collected solid was transferred to a Schlenk flask. The material was activated under high vacuum (<100 mbar) at 100 °C for 24 h, then the Schlenk flask was transferred into a N_2-filled glovebox. Activated Cu_2Cl_2(btdd) was obtained as a dark red solid. Prior to gas sorption analysis, the material was activated for an additional 24 h under high vacuum (<10 μbar) at 180 °C.

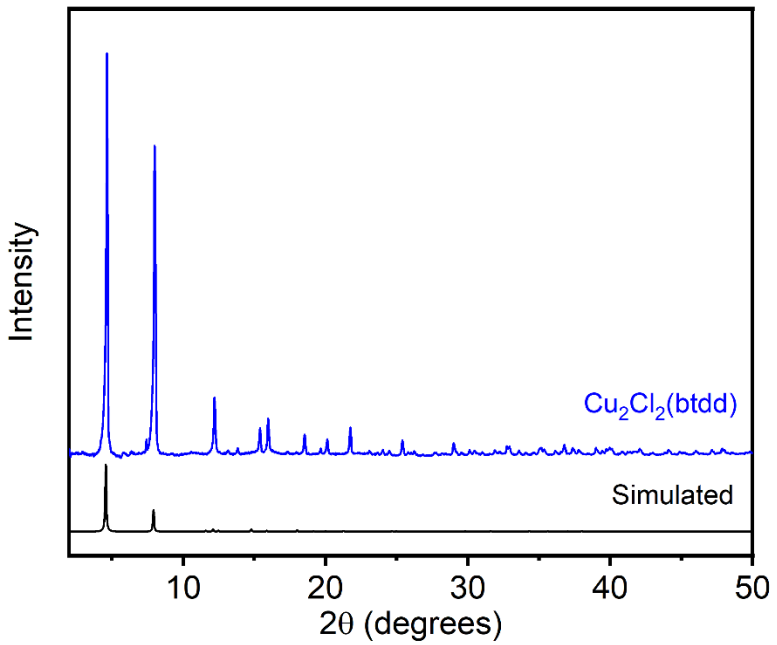

Figure S21. PXRD (λ = 1.54 Å) pattern of MeOH-solvated Cu_2Cl_2(btdd). The simulated pattern (black) based on the SCXRD structure of the isostructural MOF Mn_2Cl_2(btdd) is included for reference.[4]

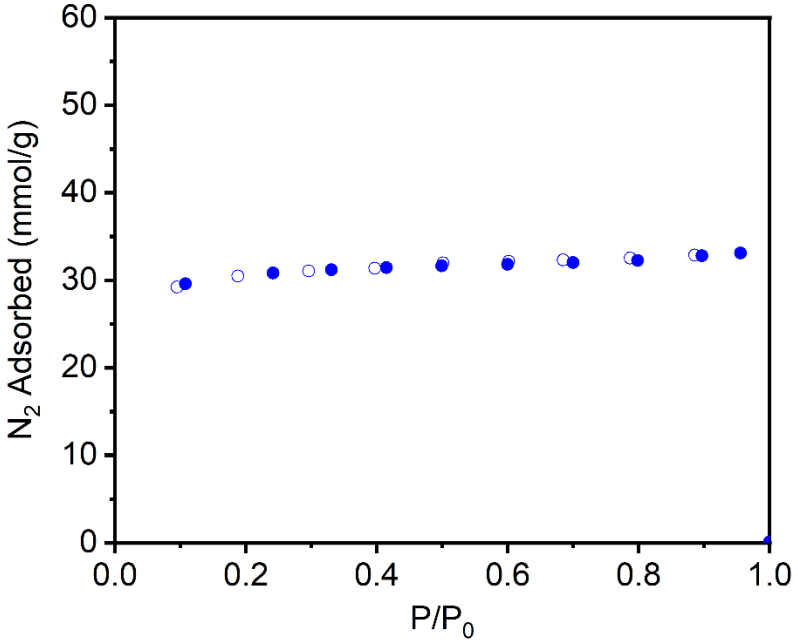

Figure S22. N_2 adsorption (solid circles) and desorption (open circles) isotherms of activated Cu_2Cl_2(btdd) at 77 K. The Langmuir surface area of this material was determined to be 3196 ± 7 m^2/g (Literature BET: 2066 m^2/g).[6]

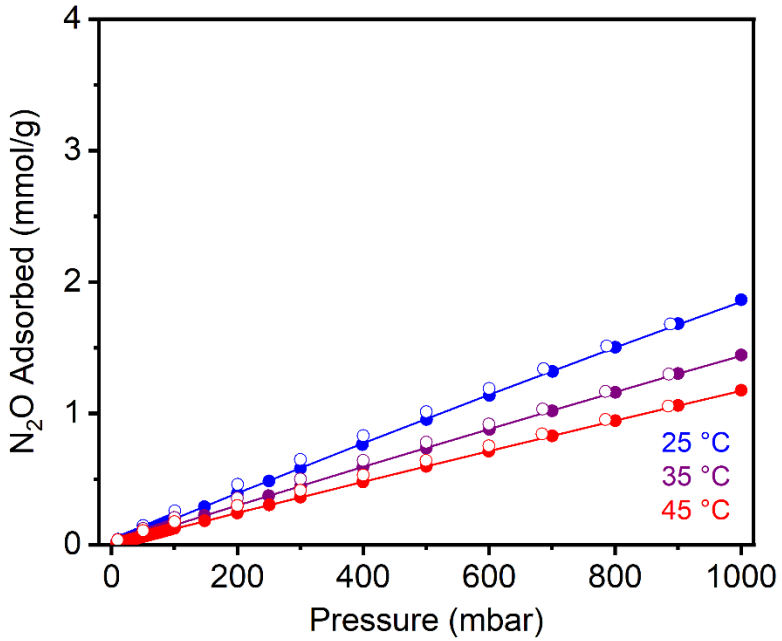

Figure S23. N_2O adsorption (solid circles) and desorption (open circles) isotherms of activated Cu_2Cl_2(btdd) at 25 °C (blue), 35 °C (purple), and 45 °C (red). Solid lines represent fits to the dual-site Langmuir-Freundlich model. The sample was reactivated at 180 ºC for 24 h under high vacuum (<10 µbar) between isotherms. A data point was considered equilibrated when less than 0.01% change in pressure occurred over a 30 or 60 s interval.

Table S4. Langmuir-Freundlich fit parameters determined from the fits in Figure S23.

	25 °C	35 °C	45 °C
$Q_{sat}1$ (mmol/g)	26.3	29.3	45.6
S1 (in multiples of R)	5.04	3.85	5.09
E1 (kJ/mol)	6.09	2.27	3.81
V1	1.00	1.00	1.00
$Q_{sat}2$ (mmol/g)	0.001	0.00	0.047
S2 (in multiples of R)	0.016	0.040	0.012
E2 (kJ/mol)	0.030	0.00	0.00
V2	1.00	1.00	1.00

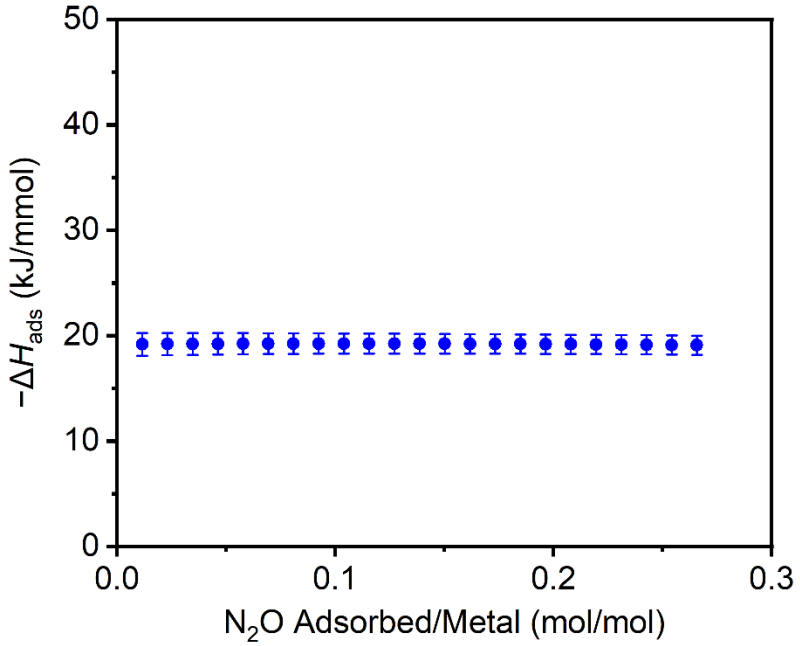

Figure S24. $-\Delta H_{ads}$ for N_2O adsorption as a function of uptake per open metal site in Cu_2Cl_2(btdd), as determined using the fits in Figure S23.

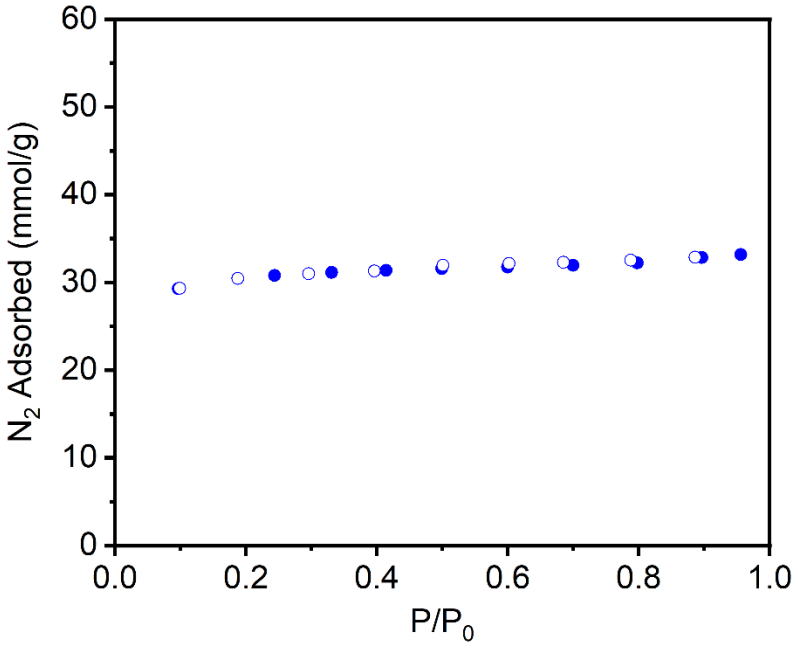

Figure S25. N_2 adsorption (solid circles) and desorption (open circles) isotherms of activated Cu_2Cl_2(btdd) at 77 K after the N_2O adsorption isotherms. The Langmuir surface area of this material was determined to be 3191 ± 8 m^2/g.

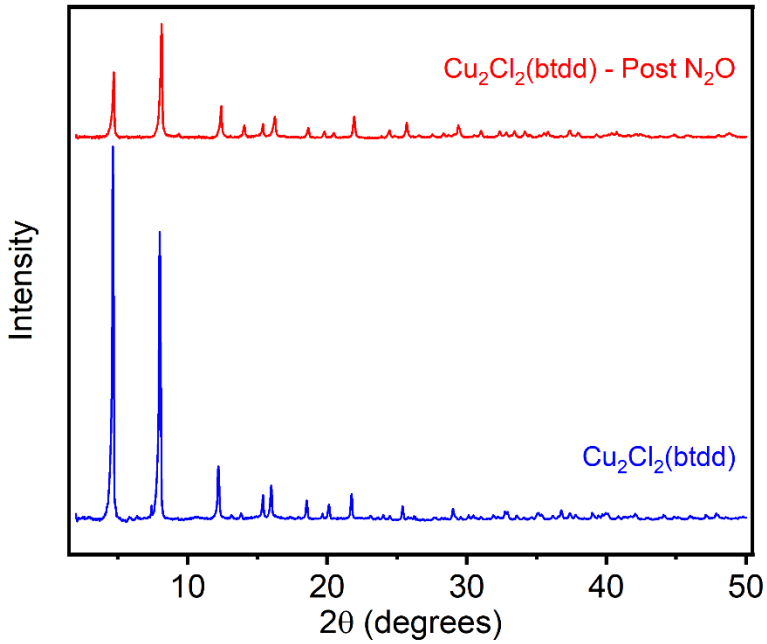

Figure S26. PXRD (λ = 1.54 Å) pattern of activated Cu_2Cl_2(btdd) after the N_2O adsorption isotherms. The experimental pattern prior to the N_2O adsorption isotherms is included for reference.

7. Synthesis, characterization, and gas sorption analysis of $Mg_2(dobdc)$.

Synthesis of $Mg_2(dobdc)$. This procedure is adapted from the literature.[7] A 1 L round bottom flask equipped with a stir bar and reflux condenser was charged with H_4dobdc (0.991 g, 5.00 mmol, 1.00 equiv.), $Mg(NO_3)_2 \cdot 6H_2O$ (3.21 g, 12.5 mmol, 2.50 equiv.), H_2O (25 mL), EtOH (25 mL), and DMF (450 mL). The reaction mixture was transferred to a silicone oil bath and stirred at reflux (700 rpm) for 24 h. After 24 h, the heterogeneous reaction mixture was allowed to cool to room temperature and filtered. The resulting solid was transferred to a 500 mL Pyrex jar with fresh DMF (250 mL). The jar was allowed to stand for 24 h at 120 °C in an oven, at which time the DMF was decanted and replaced with fresh DMF (250 mL). This procedure was repeated two additional times for a total of three hot DMF soaks. Next, the solid was filtered and returned to the jar with fresh MeOH (250 mL). The solid was soaked in MeOH for 24 h at 60 °C in an oven three total times following the same procedure as described above. Complete exchange of DMF for MeOH was confirmed by IR spectroscopy. The resulting light brown solid was filtered and transferred to a Schlenk flask. The solid was activated under flowing N_2 at 180 °C for 4 h, followed by further activation under high vacuum (<100 mbar) at 180 °C for 24 h. The Schlenk flask was transferred into a N_2-filled glovebox. Activated $Mg_2(dobdc)$ was obtained as a light brown solid. Prior to gas sorption analysis the sample was further activated under high vacuum (<10 μbar) at 180 °C for 24 h.

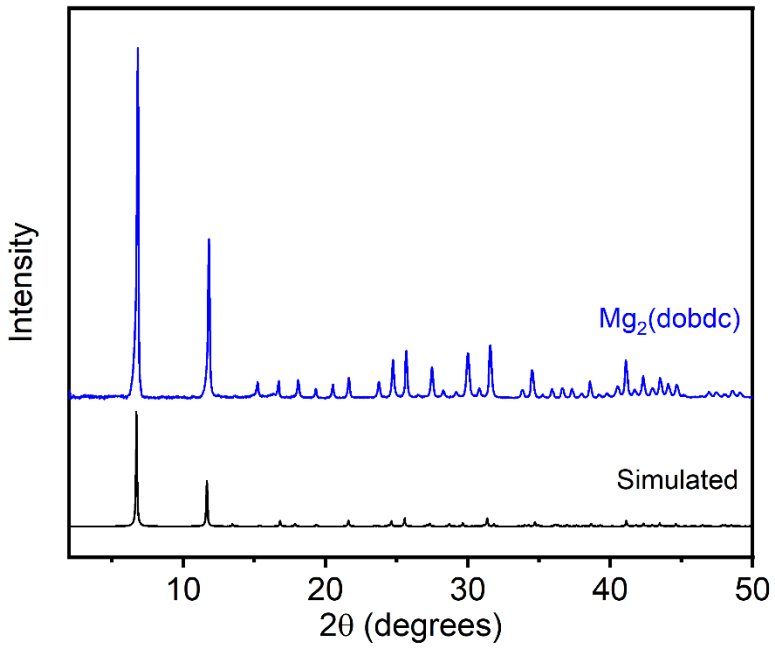

Figure S27. PXRD (λ = 1.54 Å) pattern of MeOH-solvated $Mg_2(dobdc)$. The simulated pattern (black) based on the SCXRD structure of the isostructural MOF $Zn_2(dobdc)$ is included for reference.[1]

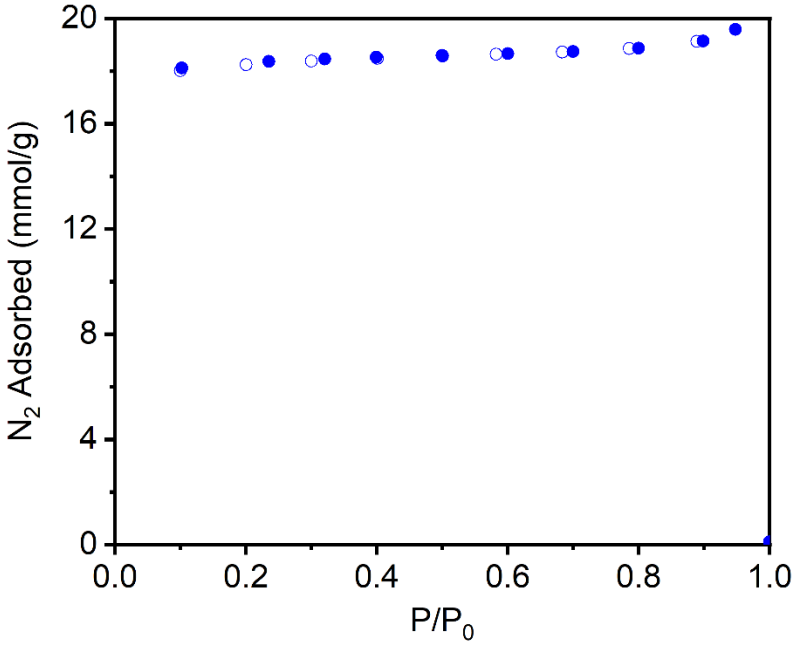

Figure S28. N_2 adsorption (solid circles) and desorption (open circles) isotherms of activated Mg_2(dobdc) at 77 K. The Langmuir surface area of this material was determined to be 1852 ± 5 m^2/g (Literature: 1957 m^2/g).[8]

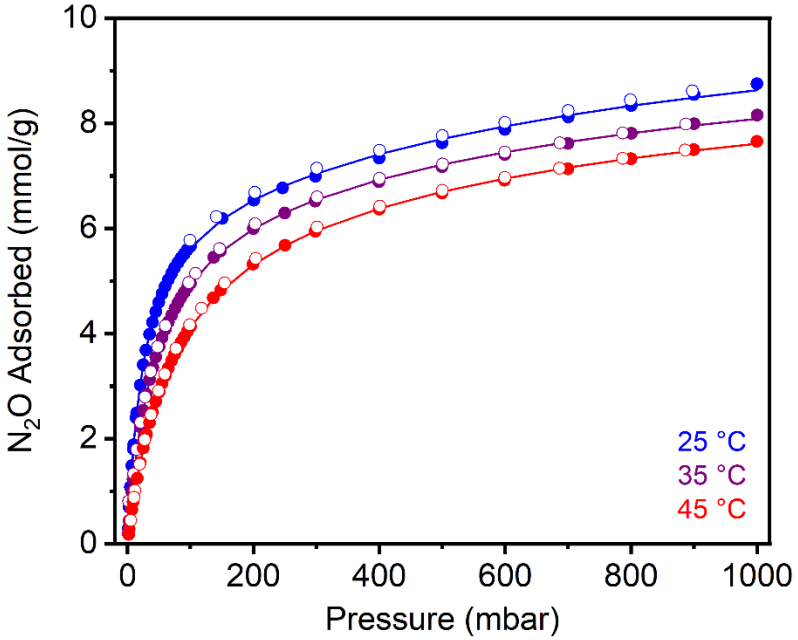

Figure S29. N_2O adsorption (solid circles) and desorption (open circles) isotherms of activated Mg_2(dobdc) at 25 °C (blue), 35 °C (purple), and 45 °C (red). Solid lines represent fits to the dual-site Langmuir-Freundlich model. The sample was reactivated at 180 ºC for 24 h under high vacuum (<10 μbar) between isotherms. A data point was considered equilibrated when less than 0.01% change in pressure occurred over a 30 or 60 s interval.

Table S5. Langmuir-Freundlich fit parameters determined from the fits in Figure S29.

	25 °C	35 °C	45 °C
$Q_{sat}1$ (mmol/g)	6.47	6.43	6.30
S1 (in multiples of R)	4.36	4.46	4.50
E1 (kJ/mol)	20.0	19.7	19.1
V1	1.00	1.00	1.00
$Q_{sat}2$ (mmol/g)	4.75	3.83	3.41
S2 (in multiples of R)	0.056	0.012	0.011
E2 (kJ/mol)	0.00	0.00	0.00
V2	1.00	1.00	1.00

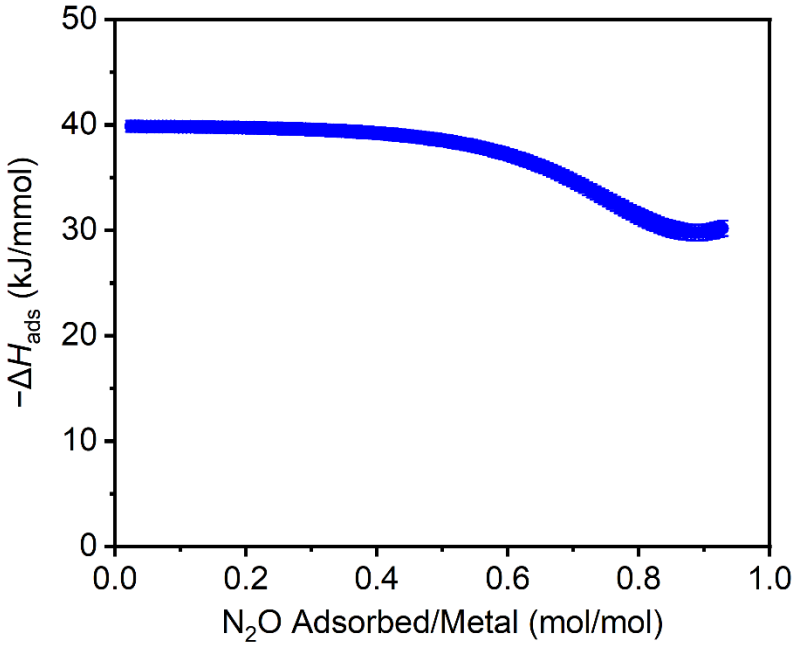

Figure S30. Heat of adsorption ($-\Delta H_{ads}$) for N_2O adsorption as a function of uptake per open metal site in Mg_2(dobdc), as determined using the fits in Figure S29.

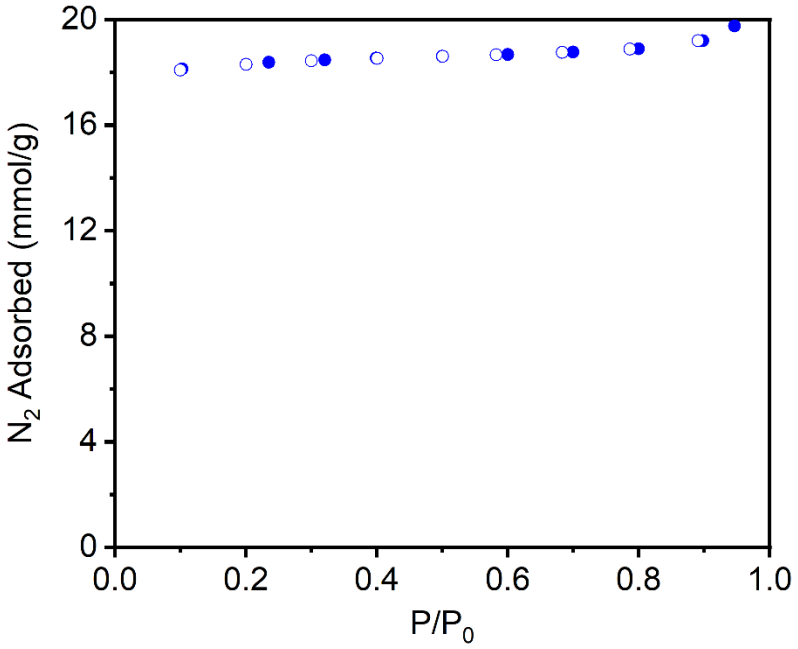

Figure S31. N_2 adsorption (solid circles) and desorption (open circles) isotherms of activated $Mg_2(dobdc)$ at 77 K after the N_2O adsorption isotherms. The Langmuir surface area of this material was determined to be 1854 ± 5 m^2/g.

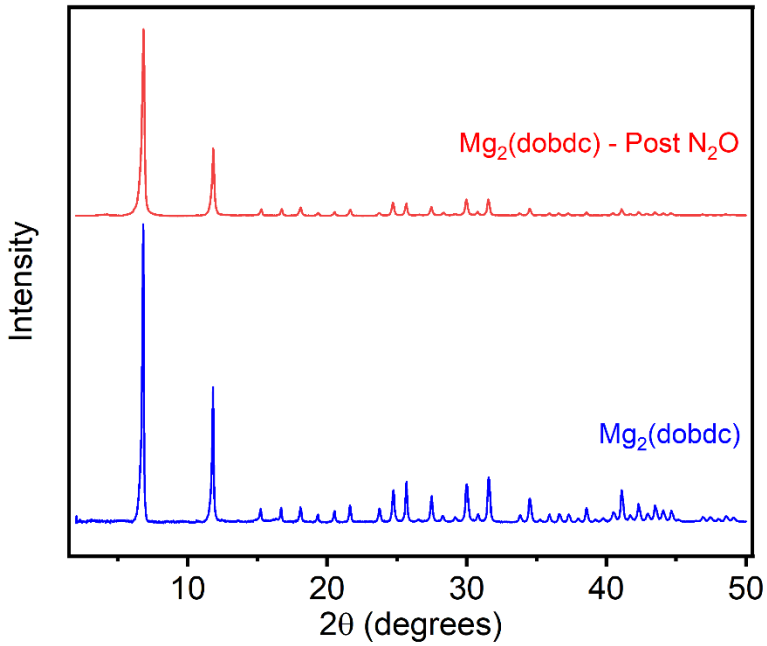

Figure S32. PXRD (λ = 1.54 Å) pattern of activated $Mg_2(dobdc)$ after the N_2O adsorption isotherms. The experimental pattern prior to the N_2O adsorption isotherms is included for reference.

8. Synthesis, characterization, and gas sorption analysis of Mn_2(dobdc).

Synthesis of Mn_2(dobdc). An air-free synthesis was developed based on previously reported procedures.[9,10] All steps of this reaction were performed under an N_2 atmosphere due to the air-sensitivity of Mn_2(dobdc). In a N_2-filled glovebox, a 350 mL screw-capped pressure vessel was charged with $MnCl_2 \cdot 4H_2O$ (5.35 g, 27.0 mmol, 4.15 eq.), H_4dobdc (1.35 g, 6.5 mmol, 1.00 eq.), dry degassed EtOH (10 mL), and dry degassed DMF (150 mL). The vessel was tightly sealed, removed from the glovebox, and placed in an oil bath. The reaction mixture was gently stirred at 135 °C for 72 h, resulting in precipitation of bright orange solid from solution. The reaction mixture was allowed to cool to room temperature, returned to the glovebox, and filtered under an atmosphere of N_2. The collected solid was returned to the 350 mL pressure vessel with fresh dry degassed DMF (150 mL). The tightly sealed vessel was placed in an oil bath and heated to 100 °C without stirring for 24 h, at which time the vessel was removed from the oil bath and returned to the glovebox. The non-homogeneous mixture was filtered and the collected solid was returned to the pressure vessel with fresh DMF (150 mL). This soaking process was repeated two more times for a total of three DMF soaks at 100 °C. After the final soak, the mixture was filtered, returned to the 350 mL pressure vessel, and the solid was suspended in MeOH (50 mL). The solid was soaked in MeOH for 24 h at 60 °C in an oil bath eight total times following the same procedure as described above. Complete exchange of DMF for MeOH was confirmed by IR spectroscopy. The mixture was filtered again, and the collected solid was transferred to a 20 mL scintillation vial equipped with a vacuum adapter. The material was activated under high vacuum (<100 mTorr) at 180 °C for 24 h in a N_2-filled glovebox. Activated Mn_2(dobdc) (0.530 g, 25.5%) was obtained as a bright orange solid. Prior to gas sorption analysis, the material was activated for an additional 24 h under high vacuum (<10 μbar) at 180 °C.

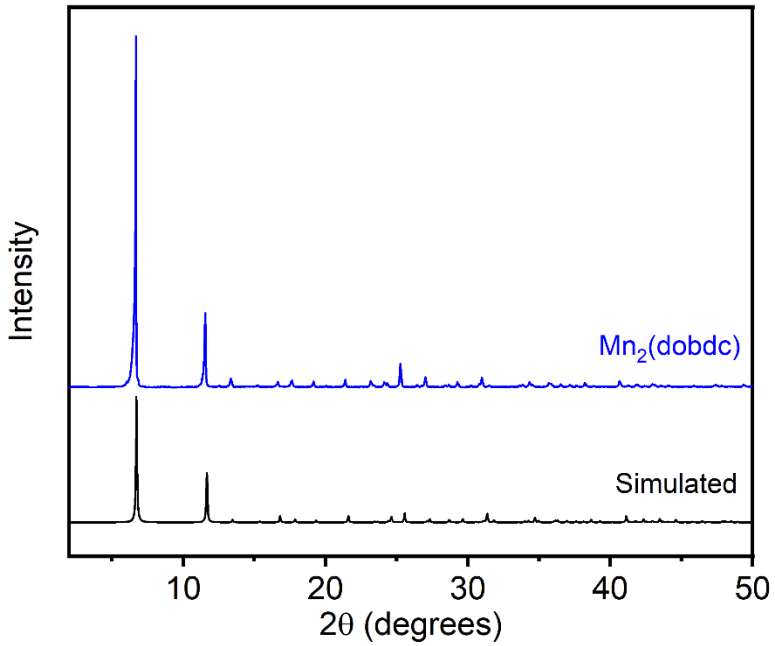

Figure S33. PXRD (λ = 1.54 Å) pattern of activated Mn_2(dobdc). The simulated pattern (black) based on the SCXRD structure of the isostructural MOF Zn_2(dobdc) is included for reference.[1]

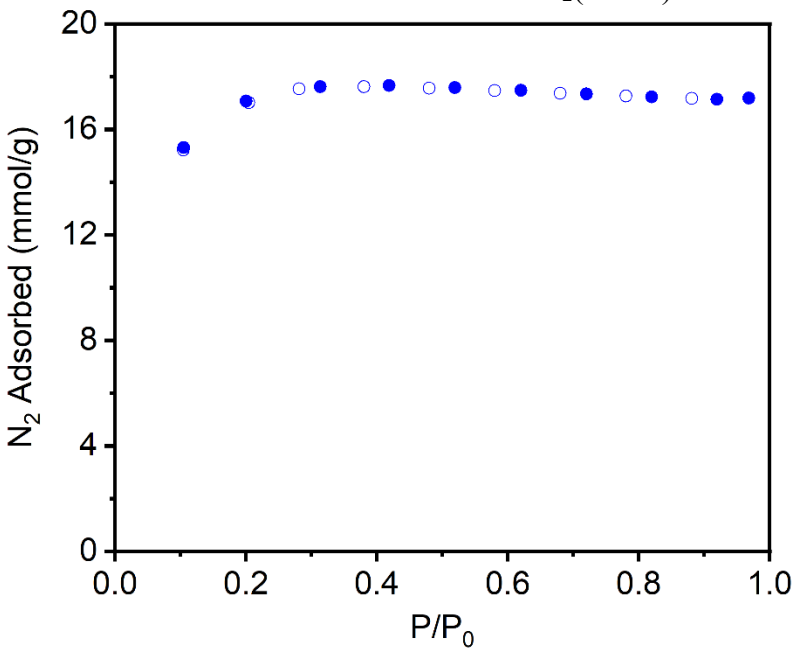

Figure S34. N_2 adsorption (solid circles) and desorption (open circles) isotherms of activated Mn_2(dobdc) at 77 K. The Langmuir surface area of this material was determined to be 1672 ± 13 m^2/g (Literature: 1797 m^2/g).[8]

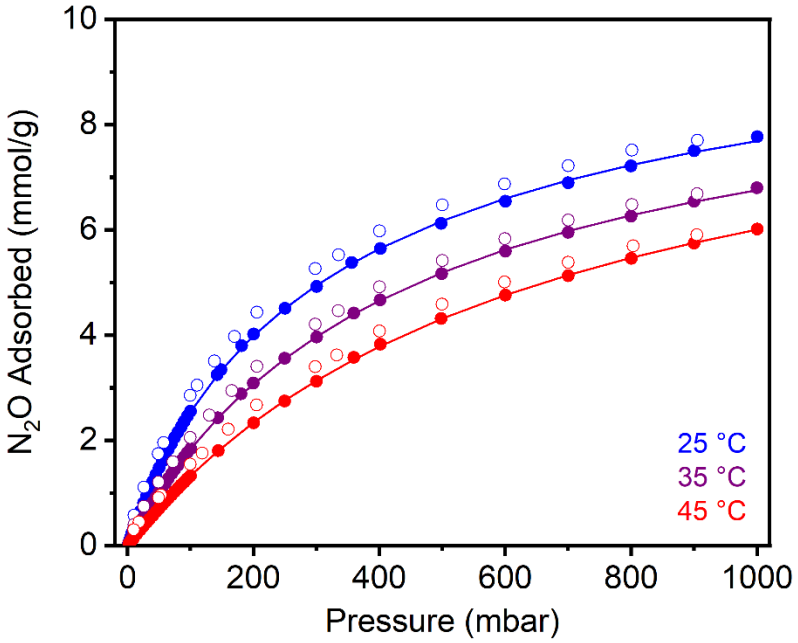

Figure S35. N_2O adsorption (solid circles) and desorption (open circles) isotherms of activated Mn_2(dobdc) at 25 °C (blue), 35 °C (purple), and 45 °C (red). Solid lines represent fits to the dual-site Langmuir-Freundlich model. The sample was reactivated at 180 ºC for 24 h under high vacuum (<10 μbar) between isotherms. A data point was considered equilibrated when less than 0.01% change in pressure occurred over a 30 or 60 s interval.

Table S6. Langmuir-Freundlich fit parameters determined from the fits in Figure S35.

	25 °C	**35 °C**	**45 °C**
Q_{sat}1 (mmol/g)	6.07	1.33	8.34
S1 (in multiples of R)	4.66	5.68	4.76
E1 (kJ/mol)	15.5	17.9	7.03
V1	1.00	1.00	1.00
Q_{sat}2 (mmol/g)	4.55	8.38	3.21
S2 (in multiples of R)	0.014	0.012	0.864
E2 (kJ/mol)	0.873	1.97	1.05
V2	1.00	1.00	1.00

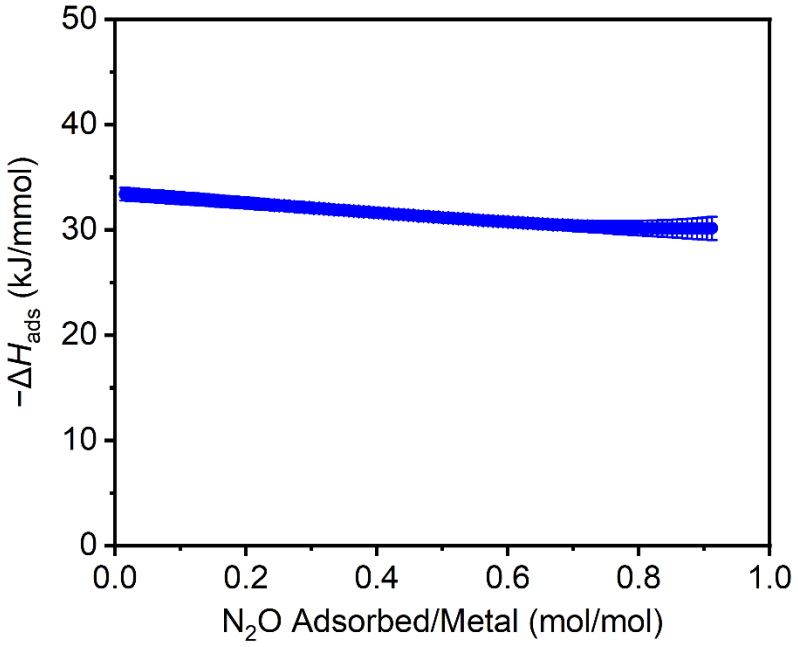

Figure S36. $-\Delta H_{ads}$ for N_2O adsorption as a function of uptake per open metal site in Mn_2(dobdc), as determined using the fits in Figure S35.

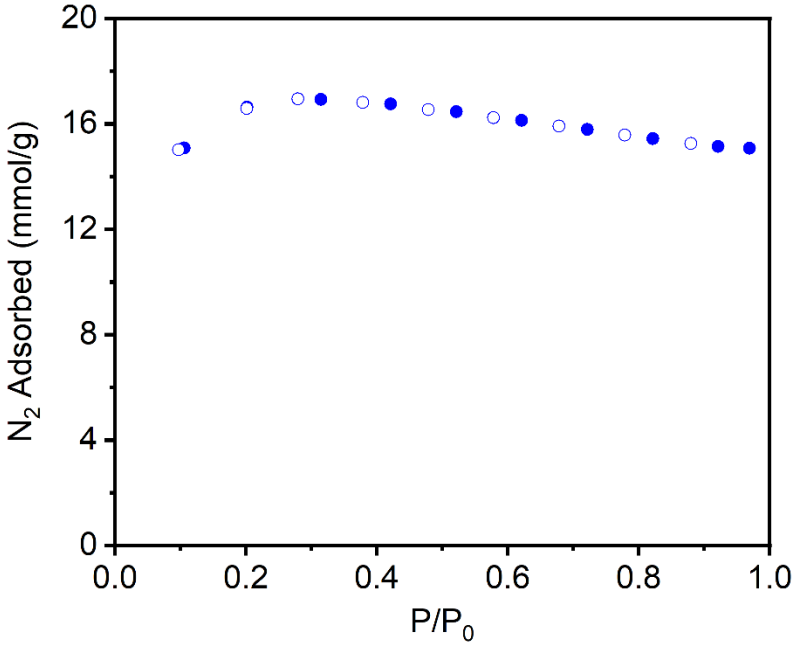

Figure S37. N_2 adsorption (solid circles) and desorption (open circles) isotherms of activated Mn_2(dobdc) at 77 K after the N_2O adsorption isotherms. The Langmuir surface area of this material was determined to be 1463 ± 25 m^2/g.

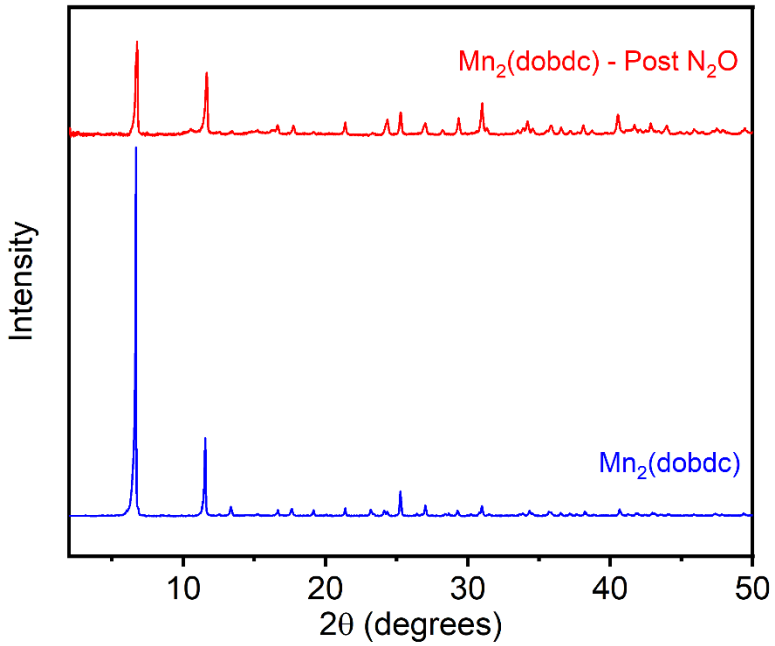

Figure S38. PXRD (λ = 1.54 Å) pattern of activated Mn_2(dobdc) after the N_2O adsorption isotherms. The experimental pattern prior to the N_2O adsorption isotherms is included for reference.

9. Synthesis, characterization, and gas sorption analysis of Fe_2(dobdc).

Synthesis of Fe_2(dobdc). Prepared according to a modified literature procedure.[11] All steps of this reaction were performed under an N_2 atmosphere due to the air-sensitivity of Fe_2(dobdc). In a N_2-filled glovebox, a 350 mL screw-cap high pressure reaction vessel equipped with a stir bar was charged with $FeCl_2$ (0.550 g, 4.50 mmol, 2.50 eq.), H_4dobdc (0.355 g, 1.80 mmol, 1.00 eq.), dry degassed DMF (150 mL), and dry degassed MeOH (18 mL). The reaction vessel was sealed, and the reaction mixture was allowed to stir slowly at 120 °C for 18 h, resulting in precipitation of an orange-red powder from solution. The reaction mixture was allowed to cool to room temperature, returned to the glovebox, and the supernatant was decanted under an atmosphere of N_2. Next, fresh dry degassed DMF (150 mL) was added. The tightly sealed vessel was removed from the glovebox, placed in an oil bath, and heated to 120 °C without stirring for 24 h, after which time the vessel was removed from the oil bath and returned to the glovebox. The supernatant was decanted under an atmosphere of N_2, then fresh dry degassed DMF (150 mL) was added to the reaction vessel. This soaking process was repeated three more times for a total of four hot DMF soaks. After the final soak, the supernatant was decanted under an atmosphere of N_2, then fresh dry degassed MeOH (150 mL) was added to the reaction vessel. The solid was soaked in MeOH for 24 h at 60 °C in an oil bath three total times following the same procedure as described above. The mixture was filtered in a N_2-filled glovebox, and the collected solid was transferred to a Schlenk flask. The material was activated under high vacuum (<100 mTorr) at 180 °C for 24 h, then the Schlenk flask was returned to the glovebox. Activated Fe_2(dobdc) was obtained as a light green solid. Prior to gas sorption analysis, the material was activated for an additional 24 h under high vacuum (<10 μbar) at 180 °C.

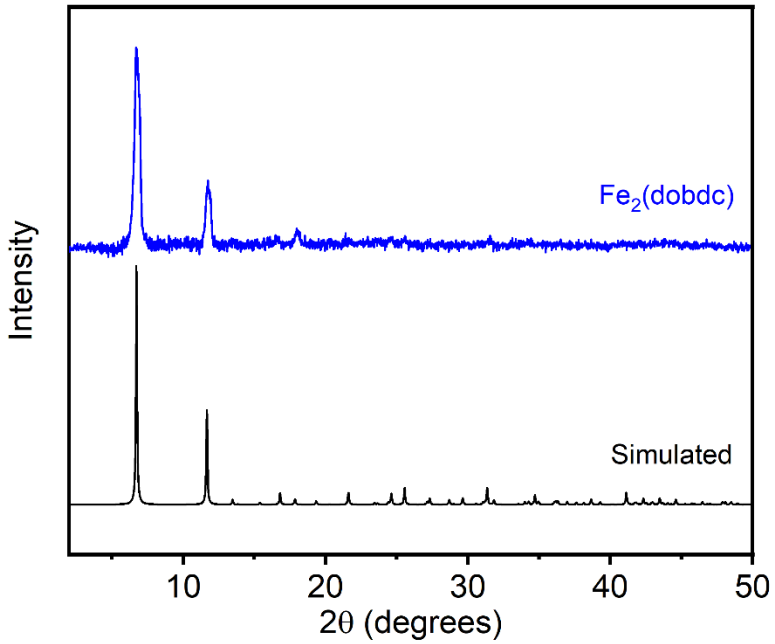

Figure S39. PXRD (λ = 1.54 Å) pattern of activated Fe_2(dobdc) measured through a glass capillary. The simulated pattern (black) based on the SCXRD structure of the isostructural MOF Zn_2(dobdc) is included for reference.[1]

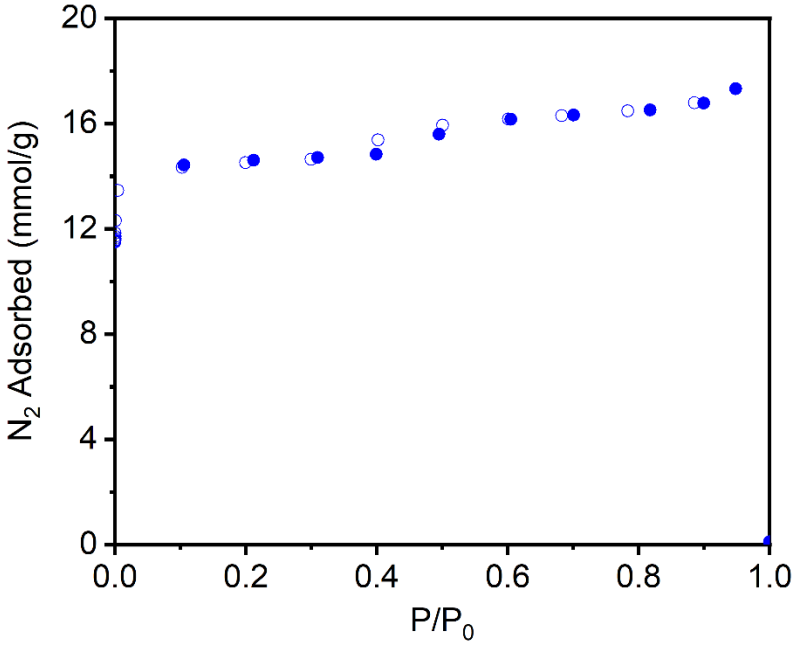

Figure S40. N_2 adsorption (solid circles) and desorption (open circles) isotherms of activated Fe_2(dobdc) at 77 K. The Langmuir surface area of this material was determined to be 1778 ± 44 m^2/g (Literature: 1536 m^2/g).[8]

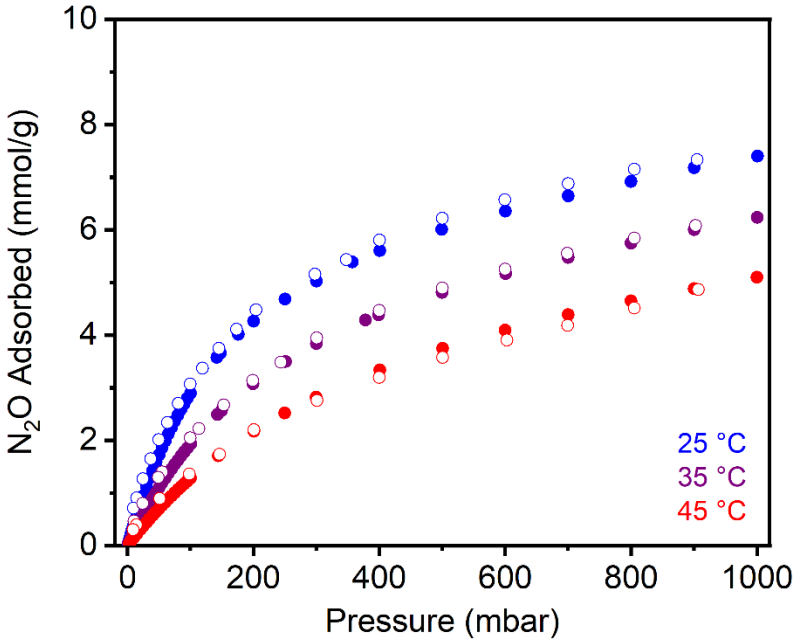

Figure S41. N_2O adsorption (solid circles) and desorption (open circles) isotherms of activated Fe_2(dobdc) at 25 °C (blue), 35 °C (purple), and 45 °C (red). The sample was reactivated at 180 ºC for 24 h under high vacuum (<10 μbar) between isotherms. A data point was considered equilibrated when less than 0.01% change in pressure occurred over a 30 of 60 s interval.

The adsorption data above were not fit to the dual-site Langmuir-Freundlich model due to the instability of Fe_2(dobdc) in the presence of N_2O under the measurement conditions. Oxidation reduces the pore volume and may contribute to framework degradation, causing the material to adsorb less gas relative to unreacted Fe_2(dobdc). These changes are not considered in the dual-site Langmuir-Freundlich model, making fits of the data unrealistic. The gradual depression of the desorption isotherms, relative to their accompanying adsorption isotherms, is consistent with gradual irreversible degradation of the MOF during the adsorption measurements. We believe that this indicates gradual oxidation of the unsaturated Fe(II) sites in the MOF by N_2O, which becomes more pronounced as the temperature increases.[12] At 45 °C, Fe_2(dobdc) incorporates less N_2O in successive measurements at nearly identical pressures, indicating that the N_2O adsorption behavior of the material has changed in response to the measurement. The gradual color change of the MOF before N_2O analysis and after each isotherm is consistent with its partial oxidation (Figure S18). Consistently, the Langmuir surface area of the material generally decreases after each successive N_2O isotherm at increasing temperatures as well (Figure S18).

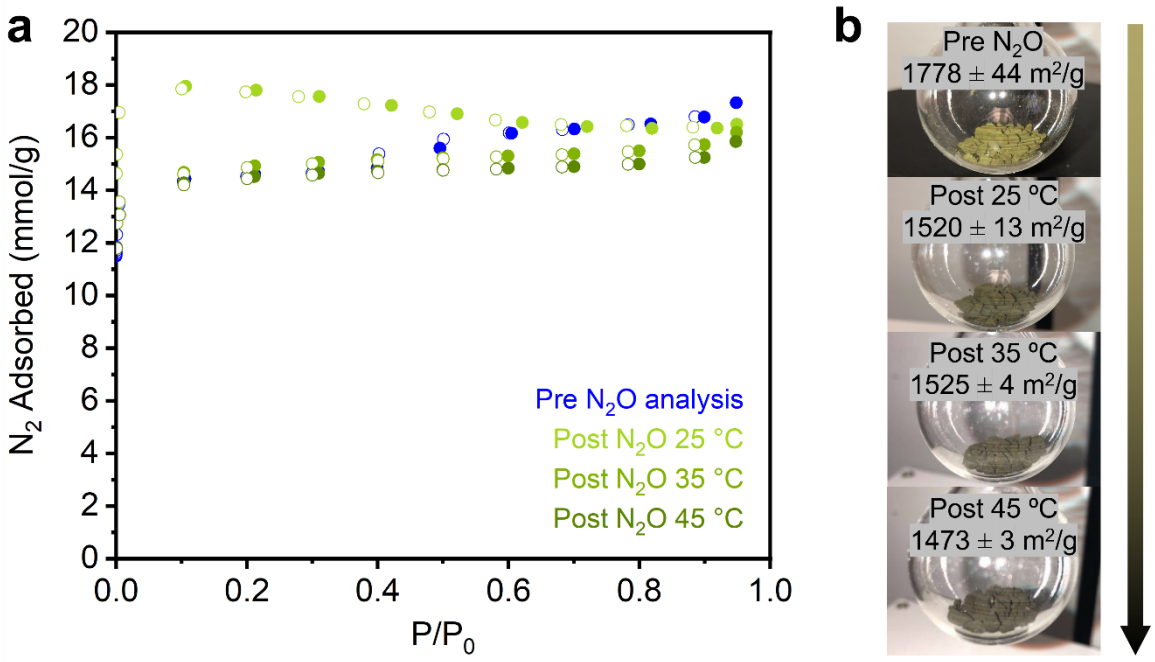

Figure S42. a) N_2 adsorption (solid circles) and desorption (open circles) isotherms of activated Fe_2(dobdc) at 77 K collected before (blue) and after N_2O adsorption isotherm measurements at 25 °C (light green), 35 °C (green), and 45 °C (dark green). The sample was reactivated at 180 ºC for 24 h under high vacuum (<10 μbar) between isotherms. b) Langmuir surface areas and images of Fe_2(dobdc) associated with each measurement.

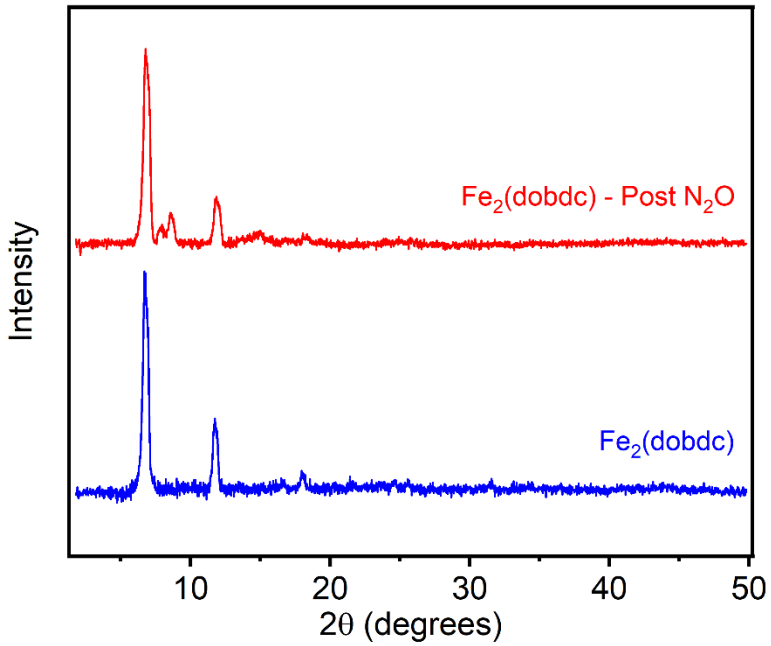

Figure S43. PXRD (λ = 1.54 Å) pattern of activated Fe_2(dobdc) after the N_2O adsorption isotherms. The experimental pattern prior to N_2O adsorption isotherms is included for reference.

10. Synthesis, characterization, and gas sorption analysis of Co_2(dobdc).

Synthesis of Co_2(dobdc). Prepared following the previously reported procedure.[13] A 1 L Pyrex jar was charged with $Co(NO_3)_2 \cdot 6H_2O$ (19.4 g, 66.7 mmol, 3.33 eq.), H_4dobdc (3.96 g, 20.0 mmol, 1.00 eq.), deionized H_2O (266 mL), DMF (266 mL), and EtOH (266 mL). The mixture was sonicated until all the solids dissolved. The jar was placed in an oven that had been pre-heated to 100 °C and allowed to stand for 24 h, resulting in precipitation of a dark purple solid from solution. The reaction mixture was allowed to cool to room temperature and filtered. The solid was quickly transferred to a 500 mL Pyrex jar filled with fresh DMF (250 mL). The jar was placed in an oven that had been pre-heated to 120 °C and left to stand 24 h, after which time the non-homogeneous mixture was filtered. The collected solid was returned to the jar with fresh DMF (250 mL). This soaking process was repeated two more times for a total of three hot DMF soaks. After the final soak, the mixture was filtered and transferred to a 500 mL Pyrex jar filled with MeOH (250 mL). The solid was soaked in MeOH for 24 h at 60 °C in an oven three total times following the same procedure as described above. The mixture was filtered again, and the collected solid was quickly transferred to a Schlenk flask under N_2. The material was activated under flowing N_2 at 180 °C for 4 h, followed by further activation under high vacuum (<100 mbar) at 180 °C for 24 h. The Schlenk flask was transferred into a N_2-filled glovebox. Activated Co_2(dobdc) (3.31 g, 53%) was obtained as a dark purple solid. Prior to gas sorption analysis, the material was activated for an additional 24 h under high vacuum (<10 μbar) at 180 °C.

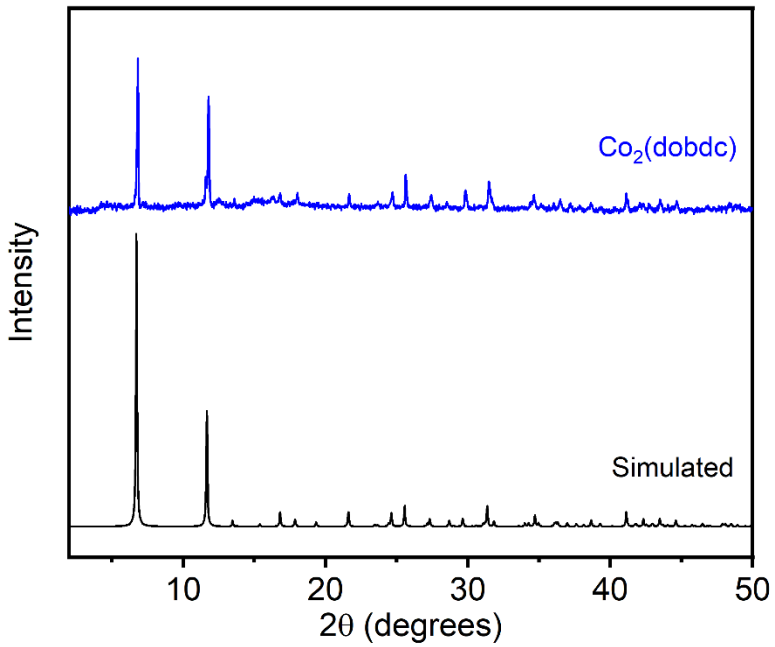

Figure S44. PXRD (λ = 1.54 Å) pattern of activated Co_2(dobdc). The simulated pattern (black) based on the SCXRD structure of the isostructural MOF Zn_2(dobdc) is included for reference.[1]

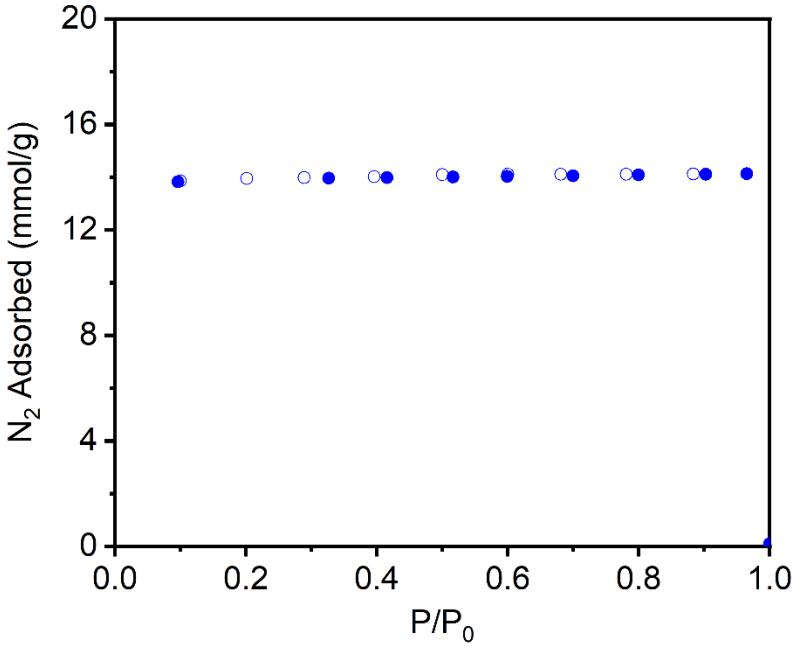

Figure S45. N_2 adsorption (solid circles) and desorption (open circles) isotherms of activated Co_2(dobdc) at 77 K. The Langmuir surface area of this material was determined to be 1377 ± 1 m^2/g (Literature: 1438 m^2/g).[8]

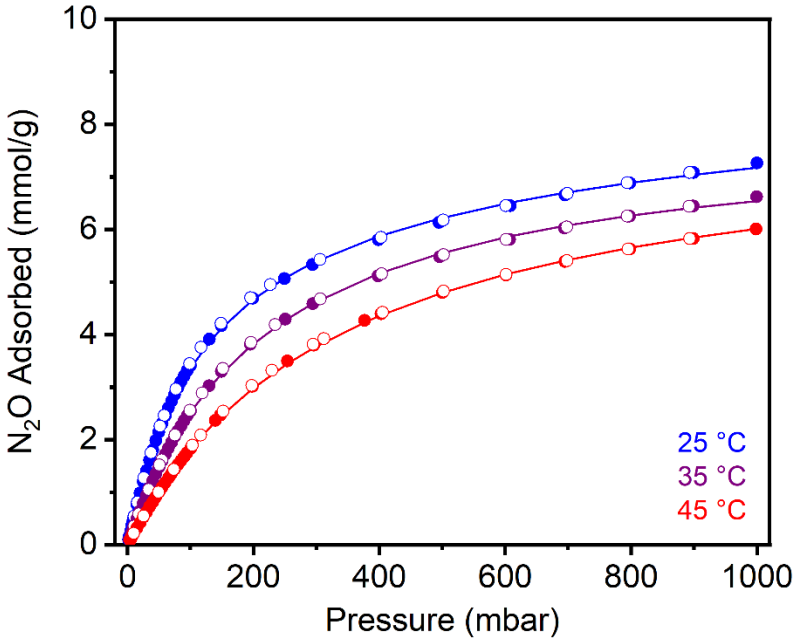

Figure S46. N_2O adsorption (solid circles) and desorption (open circles) isotherms of activated Co_2(dobdc) at 25 °C (blue), 35 °C (purple), and 45 °C (red). Solid lines represent fits to the dual-site Langmuir-Freundlich model. The sample was reactivated at 180 ºC for 24 h under high vacuum (<10 μbar) between isotherms. A data point was considered equilibrated when less than 0.01% change in pressure occurred over a 30 or 60 s interval.

Table S7. Langmuir-Freundlich fit parameters determined from the fits in Figure 46.

	25 °C	35 °C	45 °C
$Q_{sat}1$ (mmol/g)	7.00	1.30	0.925
S1 (in multiples of R)	4.46	0	4.69
E1 (kJ/mol)	16.4	3.93	15.3
V1	1.00	1.00	1.00
$Q_{sat}2$ (mmol/g)	2.65	6.65	7.13
S2 (in multiples of R)	0.655	0.012	0.011
E2 (kJ/mol)	0.00	3.96	2.88
V2	1.00	1.00	1.00

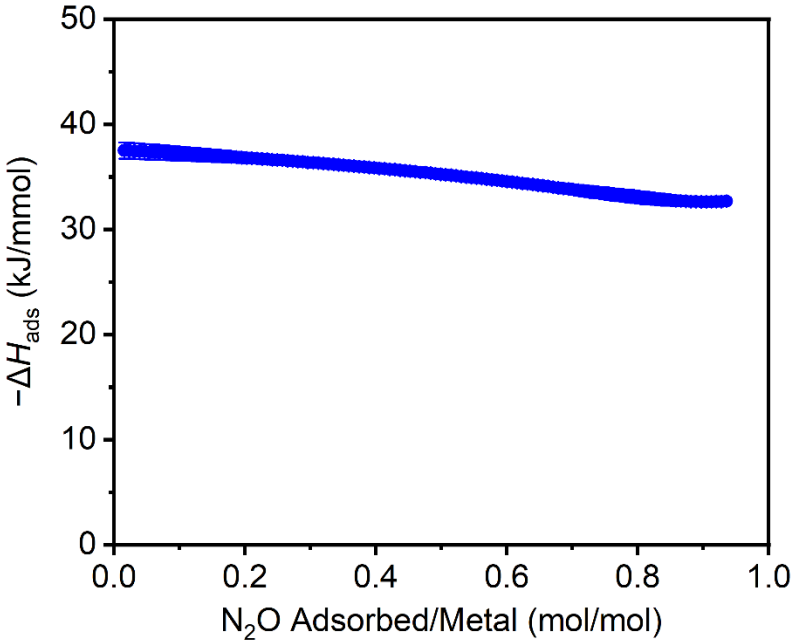

Figure S47. $-\Delta H_{ads}$ for N_2O adsorption as a function of uptake per open metal site in Co_2(dobdc), as determined using the fits in Figure S46.

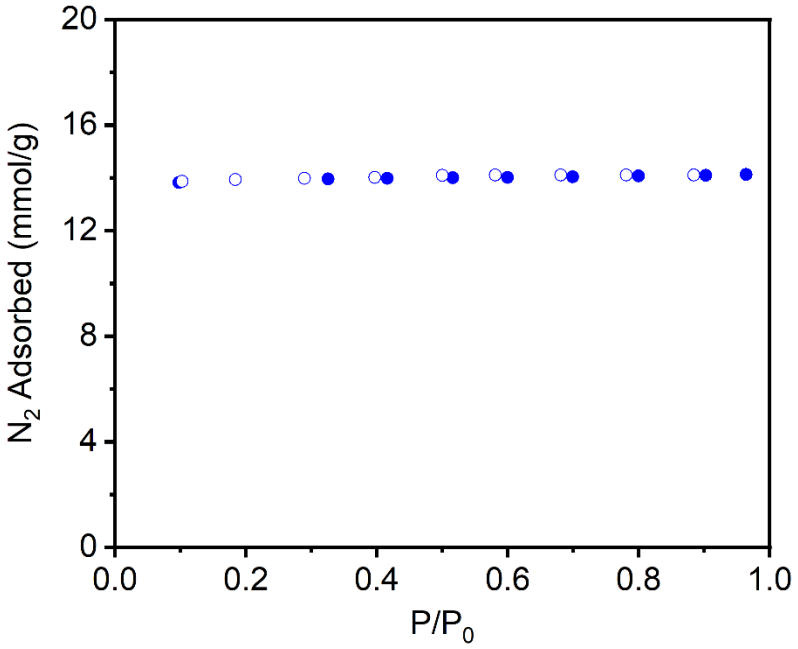

Figure S48. N_2 adsorption (solid circles) and desorption (open circles) isotherms of activated Co_2(dobdc) at 77 K after the N_2O adsorption isotherms. The Langmuir surface area of this material was determined to be 1377 ± 1 m^2/g.

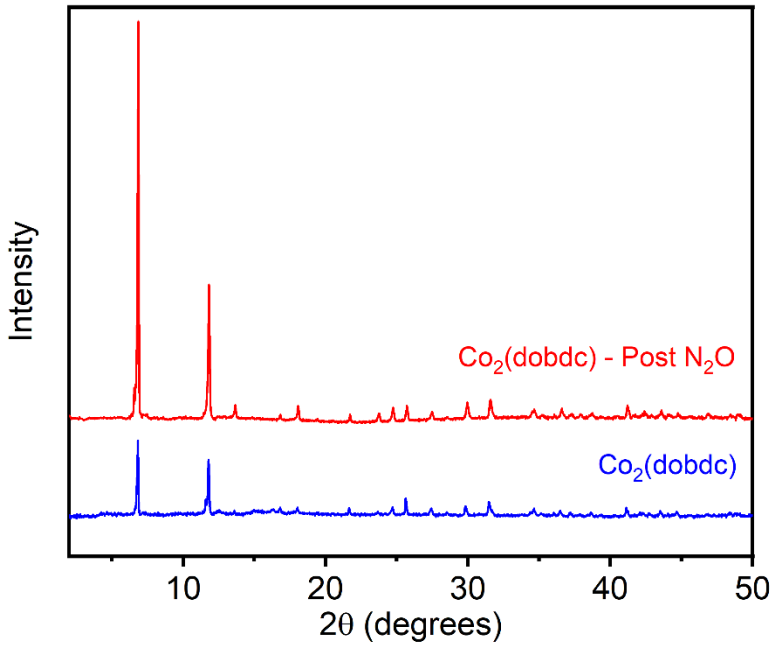

Figure S49. PXRD (λ = 1.54 Å) pattern of activated Co_2(dobdc) after the N_2O adsorption isotherms. The experimental pattern prior to N_2O adsorption isotherms is included for reference.

11. Synthesis, characterization, and gas sorption analysis of Ni_2(dobdc).

Synthesis of Ni_2(dobdc). Prepared according to a modified literature procedure.[14] A 350 mL screw-cap high pressure reaction vessel equipped with a stir bar was charged with $Ni(NO_3)_2 \cdot 6H_2O$ (5.23 g, 18.0 mmol, 2.51 eq.), H_4dobdc (1.42 g, 7.17 mmol, 1.00 eq.), fresh DMF (175 mL), and MeOH (21 mL). The mixture was sonicated until all the solids dissolved and then vigorously sparged with N_2 for 1 h. The reaction vessel was sealed, and the reaction mixture was stirred slowly at 120 °C for 14 h, resulting in precipitation of a yellow-brown solid from solution. The mixture was allowed to cool to room temperature and filtered. The collected solid was quickly transferred to a 500 mL Pyrex jar filled with fresh DMF (250 mL). The jar was placed in an oven that had been pre-heated to 100 °C and the jar was left to stand for 24 h, at which time the non-homogeneous mixture was filtered. The collected solid was returned to the jar with fresh DMF (250 mL). This soaking process was repeated two more times for a total of three hot DMF soaks. The mixture was then filtered and the collected solid was transferred to a 500 mL Pyrex jar filled with MeOH (250 mL). The solid was soaked in MeOH for 24 h at 60 °C in an oven three total times following the same procedure as described above. The mixture was filtered again, and the collected solid was quickly transferred to a Schlenk flask under N_2. The material was activated under flowing N_2 at 180 °C for 24 h, followed by further activation under high vacuum (<100 mbar) at 180 °C for 24 h. The Schlenk flask was transferred into a N_2-filled glovebox. Activated Ni_2(dobdc) (0.42 g, 33%) was obtained as a yellow solid. Prior to gas sorption analysis, the material was activated for an additional 24 h under high vacuum (<10 μbar) at 180 °C.

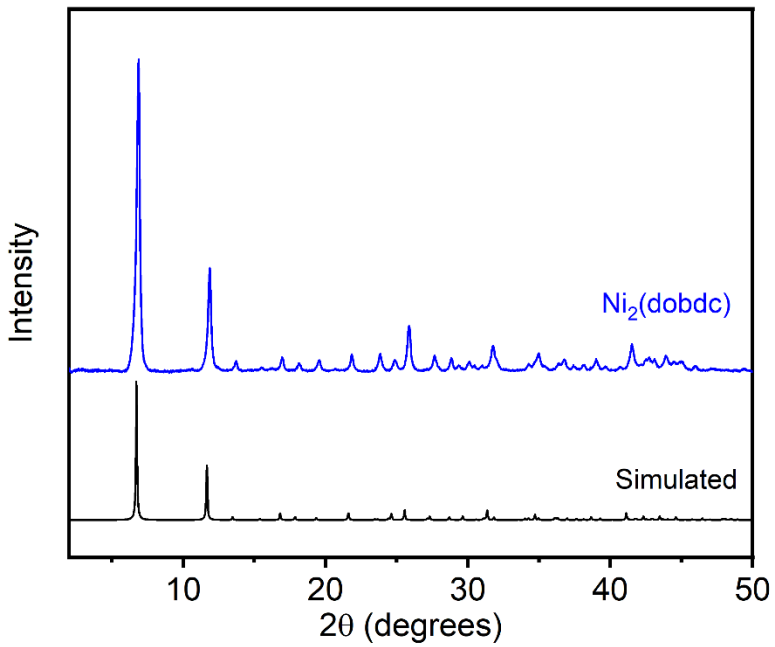

Figure S50. PXRD (λ = 1.54 Å) pattern of MeOH-solvated Ni_2(dobdc). The simulated pattern (black) based on the SCXRD structure of the isostructural MOF Zn_2(dobdc) is included for reference.[1]

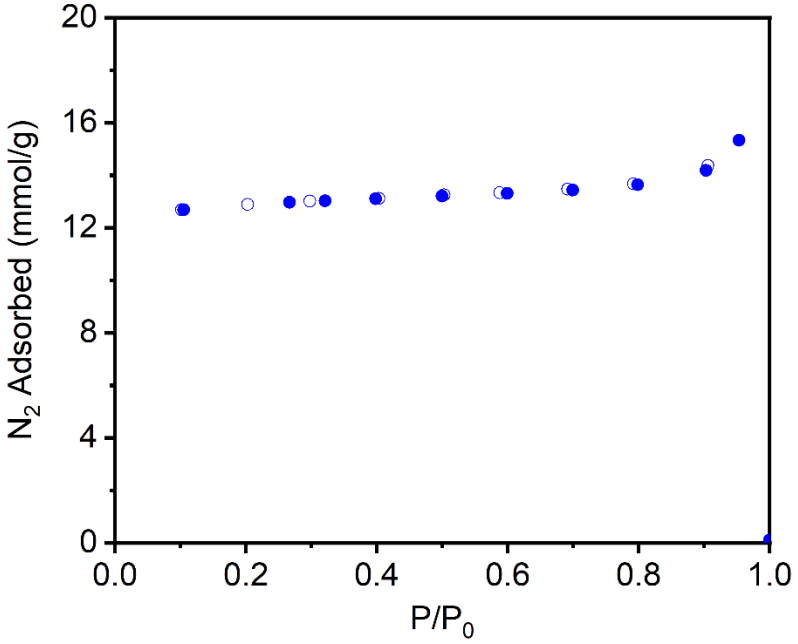

Figure S51. N_2 adsorption (solid circles) and desorption (open circles) isotherms of activated Ni_2(dobdc) at 77 K. The Langmuir surface area of this material was determined to be 1346 ± 9 m^2/g (Literature: 1574 m^2/g).[8]

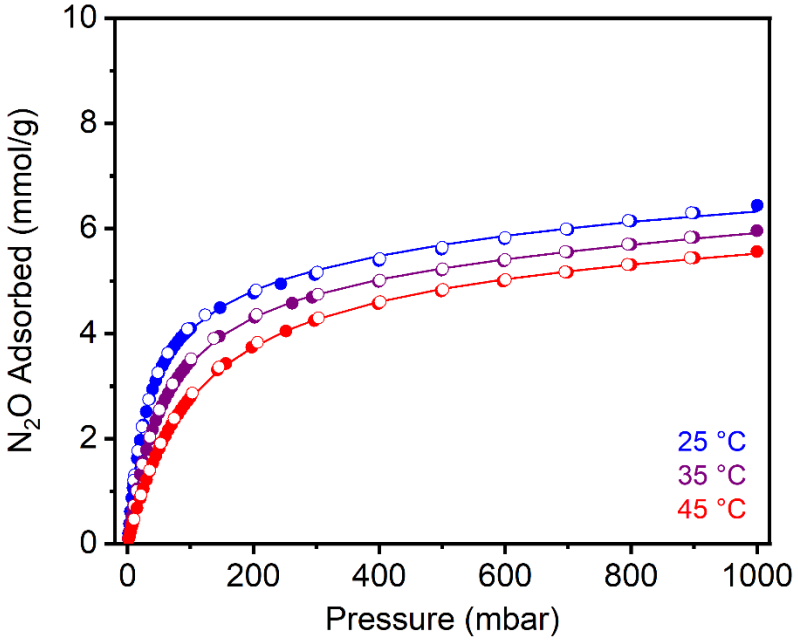

Figure S52. N_2O adsorption (solid circles) and desorption (open circles) isotherms of activated Ni_2(dobdc) at 25 °C (blue), 35 °C (purple), and 45 °C (red). Solid lines represent fits to the dual-site Langmuir-Freundlich model. The sample was reactivated at 180 ºC for 24 h under high vacuum (<10 μbar) between isotherms. A data point was considered equilibrated when less than 0.01% change in pressure occurred over a 30 or 60 s interval.

Table S8. Langmuir-Freundlich fit parameters determined from the fits in Figure S52.

	25 °C	35 °C	45 °C
$Q_{sat}1$ (mmol/g)	5.02	7.11	6.81
S1 (in multiples of R)	4.44	5.73	6.06
E1 (kJ/mol)	19.6	9.60	9.25
V1	1.00	1.00	1.00
$Q_{sat}2$ (mmol/g)	2.94	5.36	5.56
S2 (in multiples of R)	0.014	0.012	0.011
E2 (kJ/mol)	0.00	7.23	5.98
V2	1.00	1.00	1.00

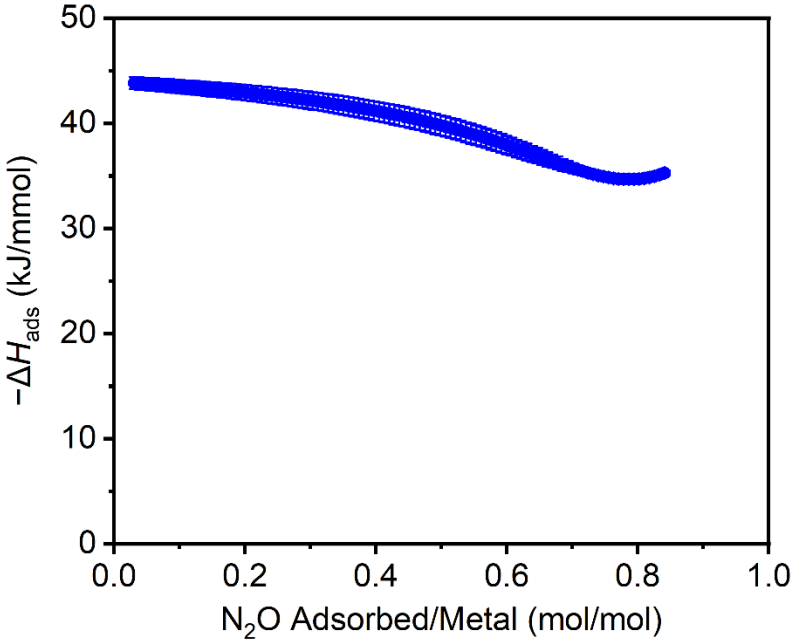

Figure S53. $-\Delta H_{ads}$ for N_2O adsorption as a function of uptake per open metal site in Ni_2(dobdc), as determined using the fits in Figure S52.

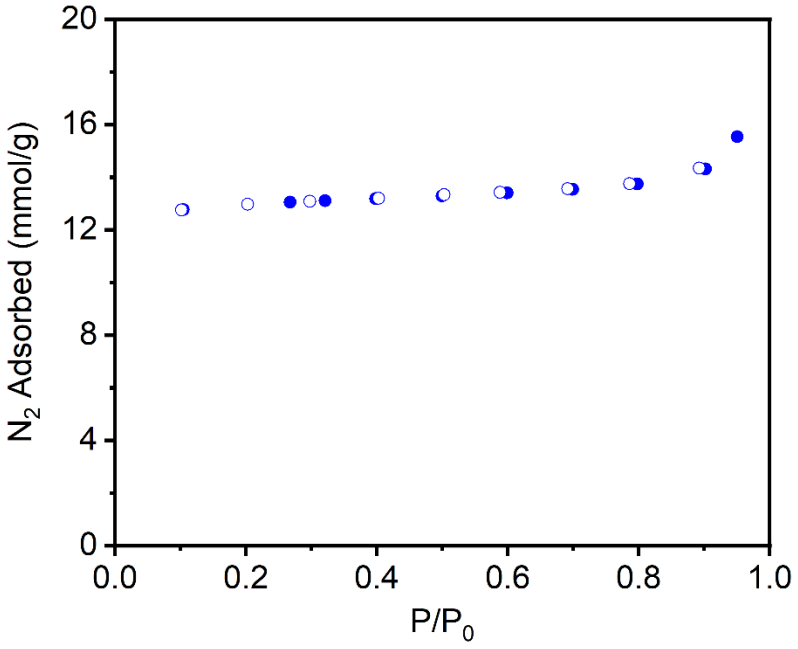

Figure S54. N_2 adsorption (solid circles) and desorption (open circles) isotherms of activated Ni_2(dobdc) at 77 K after the N_2O adsorption isotherms. The Langmuir surface area of this material was determined to be 1357 ± 9 m^2/g.

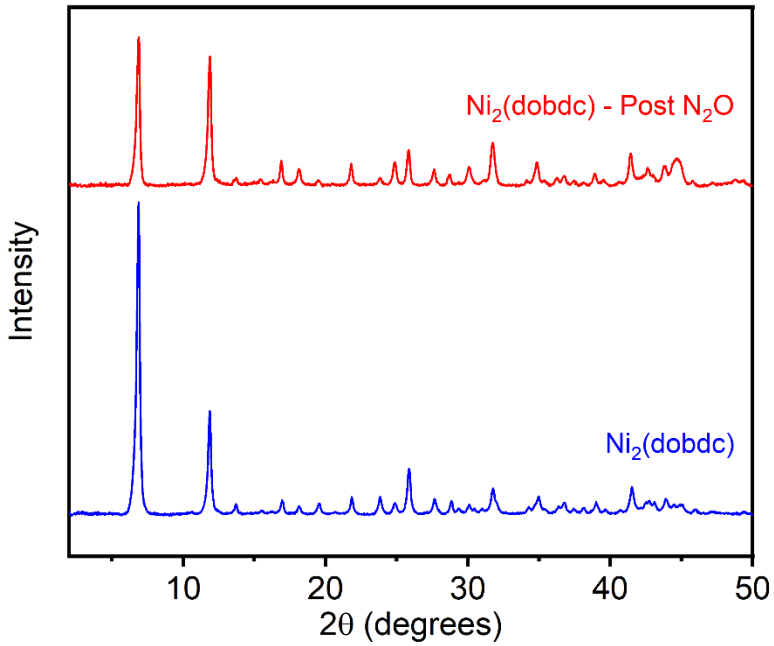

Figure S55. PXRD (λ = 1.54 Å) pattern of activated Ni_2(dobdc) after the N_2O adsorption isotherms. The experimental pattern prior to the N_2O adsorption isotherms is included for reference.

12. Synthesis, characterization, and gas sorption analysis of Cu_2(dobdc).

Synthesis of Cu_2(dobdc). Prepared according to a modified literature procedure.[8] A 75 mL screw-capped high pressure reaction vessel was charged with $Cu(NO_3)_2$•$6H_2O$ (0.445 g, 1.50 mmol, 2.50 equiv.), H_4dobdc (0.120 g, 0.60 mmol, 1.00 equiv.), *i*PrOH (24 mL), and DMF (16 mL). The mixture was sparged with N_2 for 15 min, then the vessel was capped. The mixture was sonicated until all the solids were dissolved. The vessel was placed in a pre-heated oil bath and allowed to stand at 100 °C for 1 h, resulting in the precipitation of a black powder from solution. The reaction mixture was allowed to cool to room temperature and the supernatant was removed from the settled black solid via pipette. The solid was transferred to a screw-capped jar and suspended in fresh DMF (80 mL), then the mixture was placed in an oven at 70 °C for 12 h. After this time the DMF was removed by filtration and the solids were suspended in fresh DMF (60 mL). This process was repeated five times for a total of six hot DMF soaks. The mixture was then filtered, and the solids were suspended in MeOH (80 mL) in a screw-capped jar. The solid was soaked in MeOH for 12 h at 60 °C in an oven six total times following the same procedure as described above. The mixture was then filtered, and the collected solids were transferred to a Schlenk flask. The solids were activated under flowing N_2 at 180 °C for 1 h, followed by further activation under high vacuum (<100 mbar) at 180 °C for 24 h. The solids were transferred into a N_2-filled glovebox. Activated Cu_2(dobdc) was obtained as a black solid. Prior to gas sorption analysis, the material was activated for an additional 24 h under high vacuum (<10 μbar) at 180 °C.

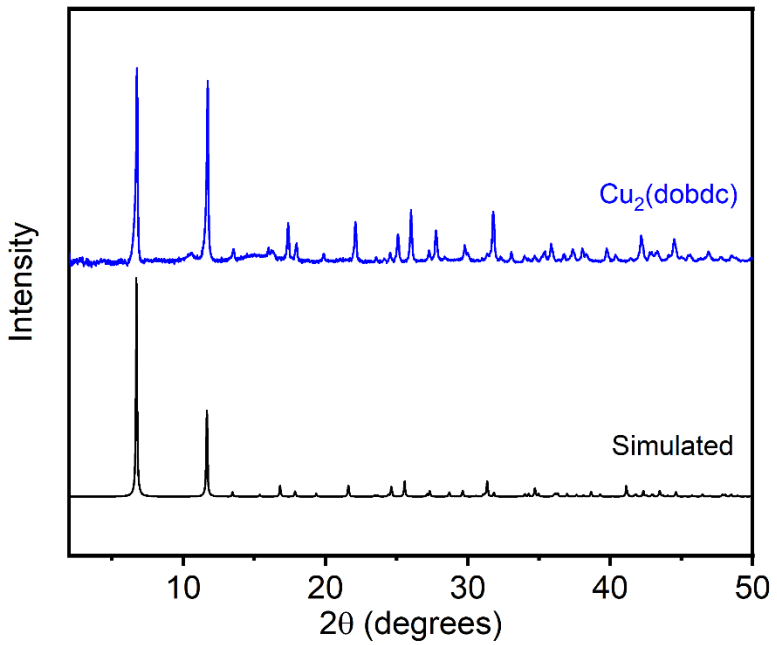

Figure S56. PXRD (λ = 1.54 Å) pattern of MeOH-solvated Cu_2(dobdc). The simulated pattern (black) based on the SCXRD structure of the isostructural MOF Zn_2(dobdc) is included for reference.[1]

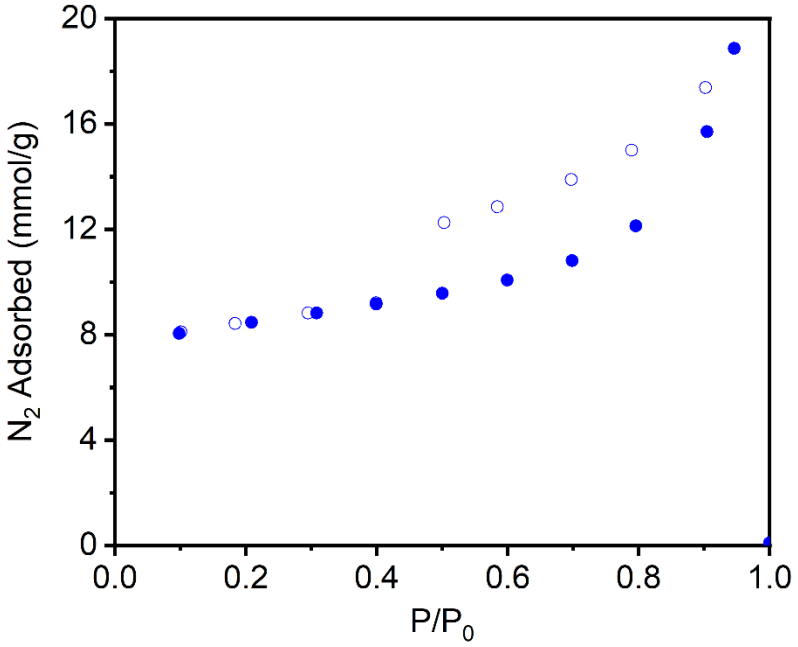

Figure S57. N_2 adsorption (solid circles) and desorption (open circles) isotherms of activated Cu_2(dobdc) at 77 K. The Langmuir surface area of this material was determined to be 1271 ± 81 m^2/g (Literature: 1515 m^2/g).[8]

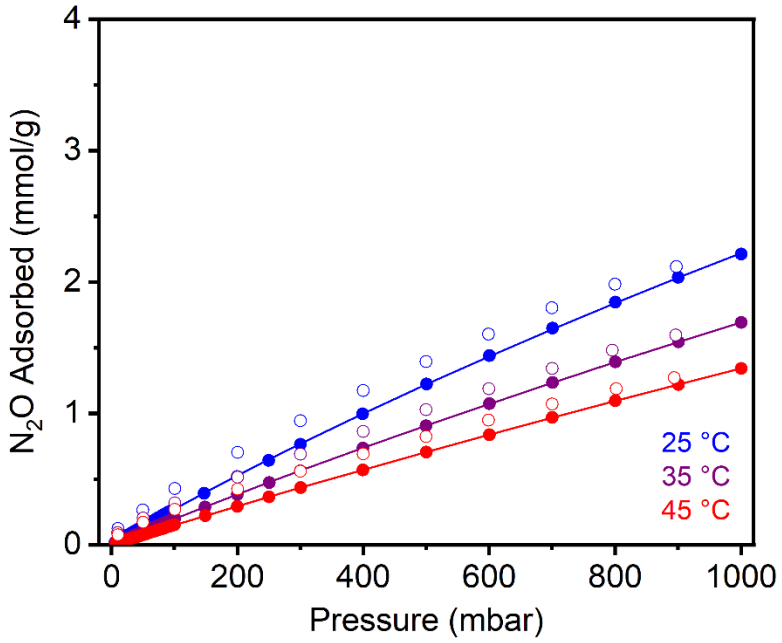

Figure S58. N_2O adsorption (solid circles) and desorption (open circles) isotherms of activated Cu_2(dobdc) at 25 °C (blue), 35 °C (purple), and 45 °C (red). Solid lines represent fits to the dual-site Langmuir-Freundlich model. The sample was reactivated at 180 ºC for 24 h under high vacuum (<10 μbar) between isotherms. A data point was considered equilibrated when less than 0.01% change in pressure occurred over a 30 or 60 s interval.

Table S9. Langmuir-Freundlich fit parameters determined from the fits in Figure S58.

	25 °C	35 °C	45 °C
$Q_{sat}1$ (mmol/g)	24.3	24.6	24.8
S1 (in multiples of R)	6.99	7.02	7.06
E1 (kJ/mol)	10.9	10.9	10.9
V1	1.00	1.00	1.00
$Q_{sat}2$ (mmol/g)	1.07	0.481	0.236
S2 (in multiples of R)	0.098	0.027	0.021
E2 (kJ/mol)	0.00	0.00	0.00
V2	1.00	1.00	1.00

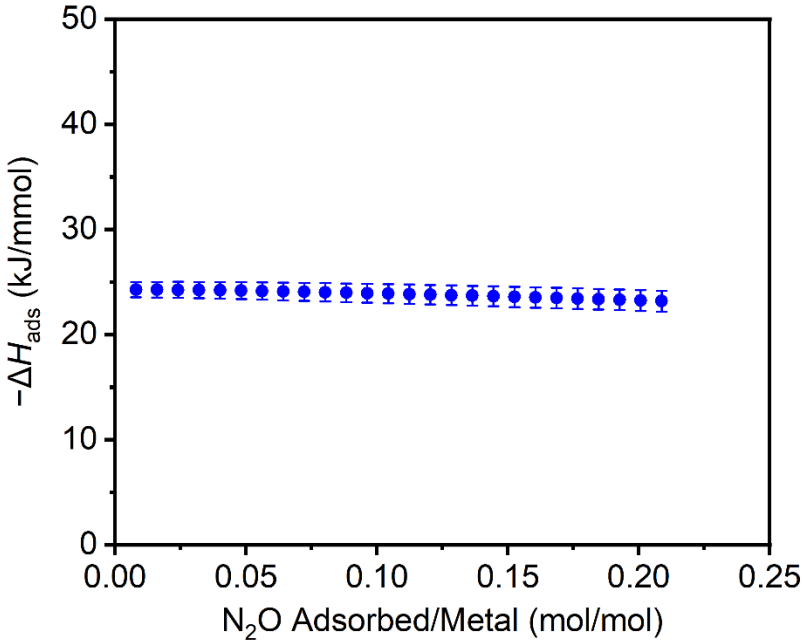

Figure S59. $-\Delta H_{ads}$ for N_2O adsorption as a function of uptake per open metal site in Cu_2(dobdc), as determined using the fits in Figure S58.

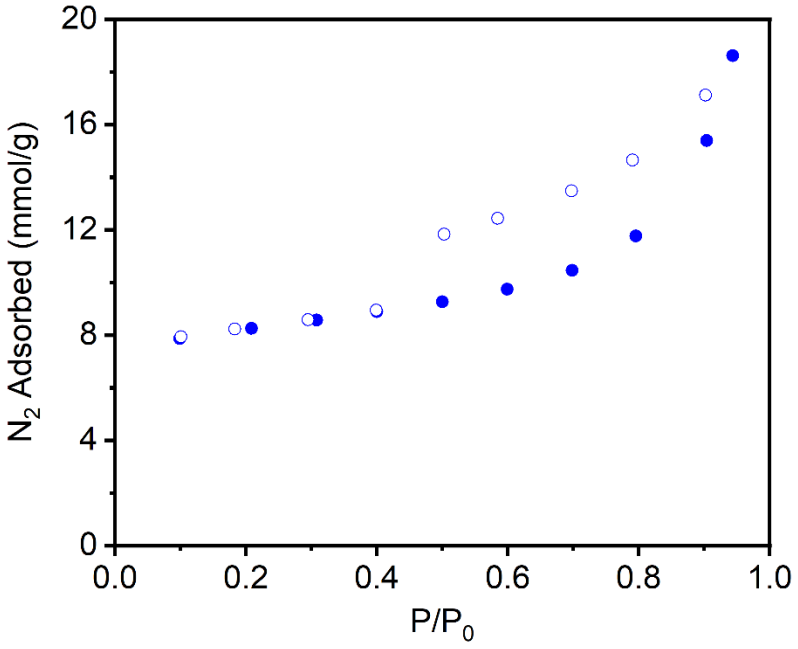

Figure S60. N_2 adsorption (solid circles) and desorption (open circles) isotherms of activated Cu_2(dobdc) at 77 K after the N_2O adsorption isotherms. The Langmuir surface area of this material was determined to be 1225 ± 79 m^2/g.

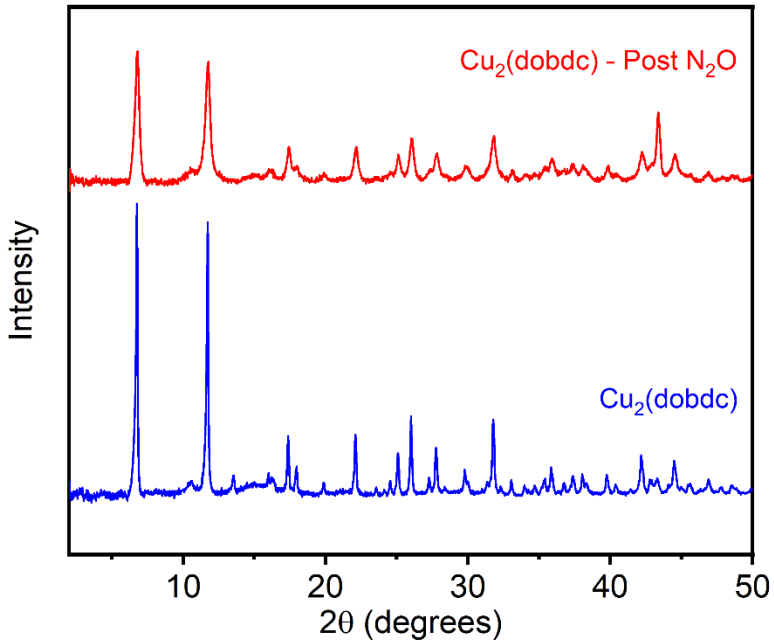

Figure S61. PXRD (λ = 1.54 Å) pattern of activated Cu_2(dobdc) after the N_2O adsorption isotherms. The experimental pattern prior to the N_2O adsorption isotherms is included for reference.

13. Synthesis, characterization, and gas sorption analysis of Zn_2(dobdc).

Synthesis of Zn_2(dobdc). Prepared according to a modified literature procedure.[7] A 350 mL screw-cap high pressure reaction vessel equipped with a stir bar was charged with $Zn(NO_3)_2 \cdot 6H_2O$ (2.23 g, 7.50 mmol, 3.00 eq.), H_4dobdc (0.495 g, 2.50 mmol, 1.00 eq.), DMF (125 mL), and EtOH (125 mL). The mixture was sonicated until all the solids dissolved. The reaction mixture was vigorously sparged with N_2 for 1 h. The reaction vessel was sealed, and the reaction mixture was stirred slowly at 120 °C for 14 h, resulting in precipitation of a yellow powder from solution. The reaction mixture was allowed to cool to room temperature and filtered. The collected solid was quickly transferred to a 500 mL Pyrex jar filled with DMF (250 mL). The jar was placed in an oven that had been pre-heated to 120 °C and left to stand for 24 h, after which time the non-homogeneous mixture was filtered. The collected solid was returned to the jar with fresh DMF (250 mL). This soaking process was repeated two more times for a total of three hot DMF soaks. The mixture was then filtered, and the solids were transferred to a 500 mL Pyrex jar filled with MeOH (250 mL). The solid was soaked in MeOH for 24 h at 60 °C in an oven three total times following the same procedure as described above. The mixture was filtered, and the collected solid was quickly transferred to a Schlenk flask under N_2. The material was activated under flowing N_2 at 180 °C for 24 h, followed by further activation under high vacuum (<100 mbar) at 180 °C for 24 h. The Schlenk flask was transferred into a N_2-filled glovebox. Activated Zn_2(dobdc) (0.799 g, 64%) was obtained as a yellow solid. Prior to gas sorption analysis, the material was activated for an additional 24 h under high vacuum (<10 μbar) at 180 °C.

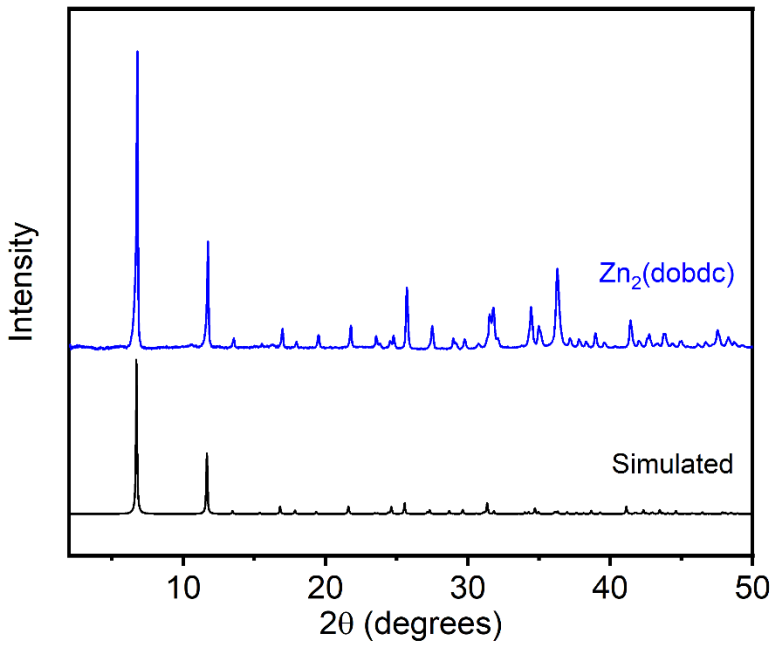

Figure S62. PXRD (λ = 1.54 Å) pattern of MeOH-solvated Zn_2(dobdc). The simulated pattern (black) based on the SCXRD structure of Zn_2(dobdc) is included for reference.[1]

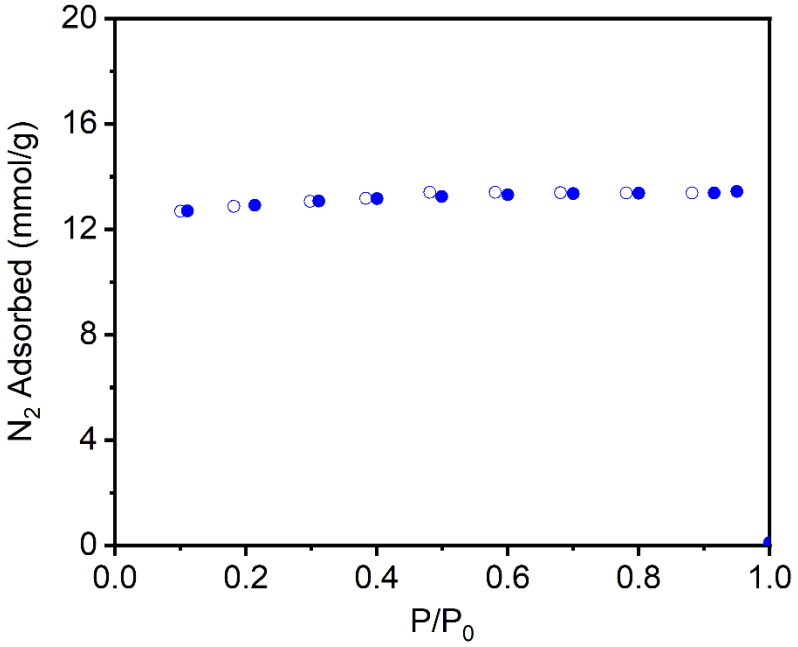

Figure S63. N_2 adsorption (solid circles) and desorption (open circles) isotherms of activated Zn_2(dobdc) at 77 K. The Langmuir surface area of this material was determined to be 1328 ± 2 m^2/g (Literature: 1277 m^2/g).[8]

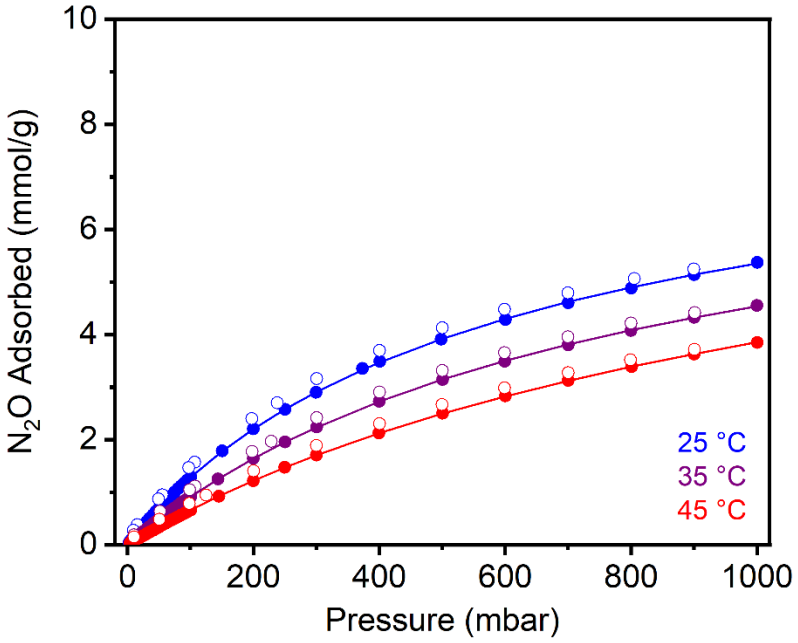

Figure S64. N_2O adsorption (solid circles) and desorption (open circles) isotherms of activated Zn_2(dobdc) at 25 °C (blue), 35 °C (purple), and 45 °C (red). Solid lines represent fits to the dual-site Langmuir-Freundlich model. The sample was reactivated at 180 °C for 24 h under high vacuum (<10 μbar) between isotherms. A data point was considered equilibrated when less than 0.01% change in pressure occurred over a 30 or 60 s interval.

Table S10. Langmuir-Freundlich fit parameters determined from the fits in Figure S64.

	25 °C	35 °C	45 °C
Q_{sat}1 (mmol/g)	4.18	3.32	3.51
S1 (in multiples of R)	4.54	6.48	4.50
E1 (kJ/mol)	13.5	6.81	7.64
V1	1.00	1.00	1.00
Q_{sat}2 (mmol/g)	4.54	7.94	6.58
S2 (in multiples of R)	0.042	0.012	0.012
E2 (kJ/mol)	0.306	0.672	0.00
V2	1.00	1.00	1.00

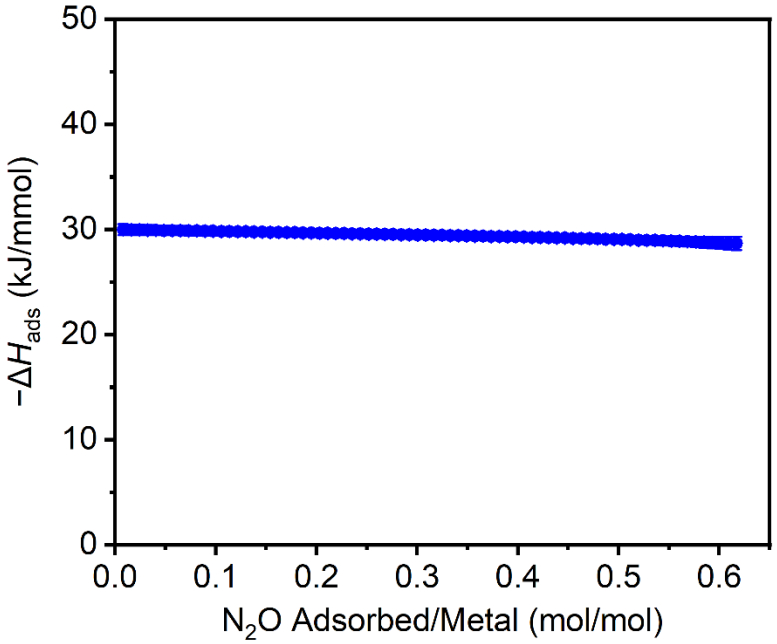

Figure S65. $-\Delta H_{ads}$ for N_2O adsorption as a function of uptake per open metal site in Zn_2(dobdc), as determined using the fits in Figure S64.

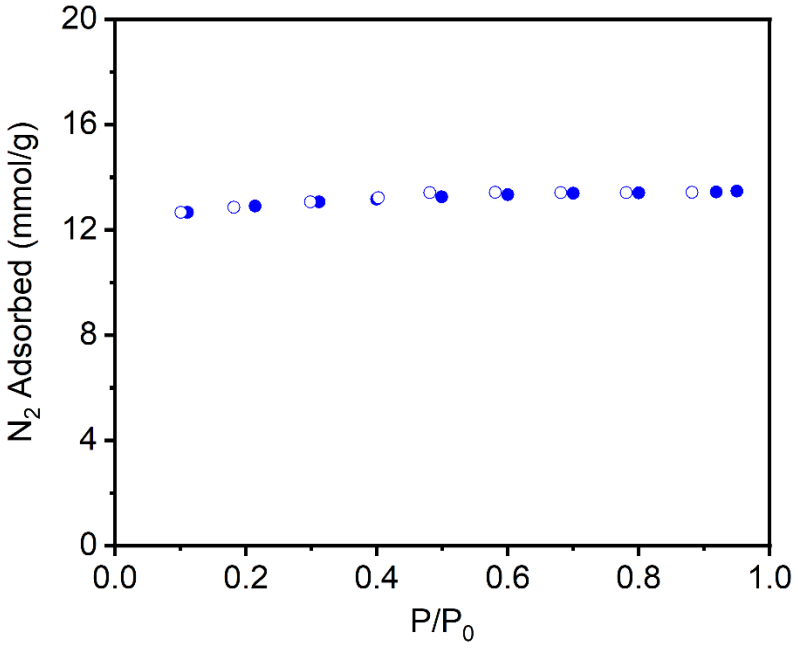

Figure S66. N_2 adsorption (solid circles) and desorption (open circles) isotherms of activated Zn_2(dobdc) after at 77 K after the N_2O adsorption isotherms. The Langmuir surface area of this material was determined to be 1334 ± 2 m^2/g.

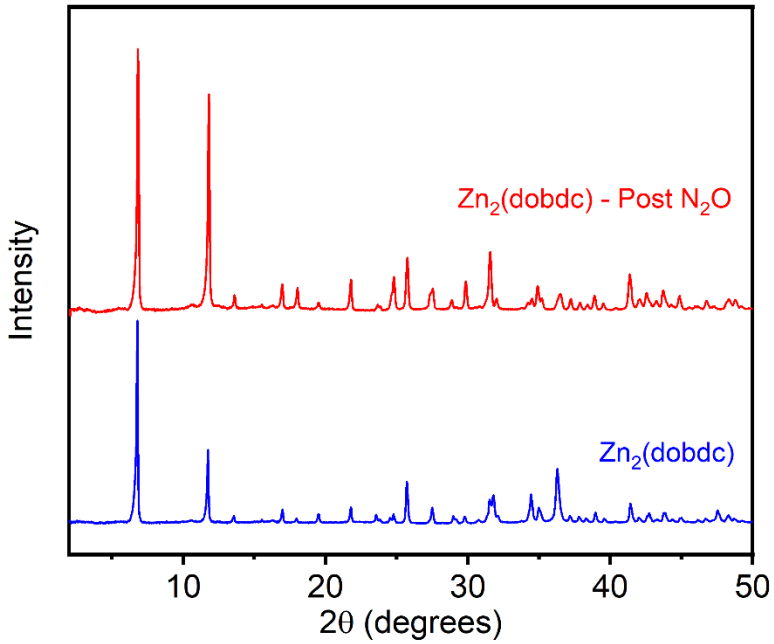

Figure S67. PXRD (λ = 1.54 Å) pattern of activated Zn_2(dobdc) after the N_2O adsorption isotherms. The experimental pattern prior to the N_2O adsorption isotherms is included for reference.

14. Computational studies.

Gas-phase geometry optimizations of MOF cluster models in this work were geometry optimized with density functional theory (DFT) using ORCA v4.0.1.2.[15] The B3LYP[16] global hybrid functional with the empirical D3 dispersion correction[17,18] incorporating the default Becke-Johnson damping was used for all models. Scalar relativistic effects were incorporated by using the zero-order regular approximation (ZORA)[19] with defaults applied in ORCA. All systems were treated as neutral with all M(II) ions in the high-spin state. All metal ions were modelled with the ZORA-def2-TZVPP[20] basis, with all remaining atoms treated with a ZORA-def2-SVP basis. We constrained the position of O atoms in linkers and allowed all other atoms to relax. All calculations made use of the resolution of identity (RI) and chain of sphere (COSX) approximations[21] to accelerate the calculations. We considered two types of spin flips (i.e., at the central metal or in one edge metal) in broken symmetry DFT (BS-DFT)[22] of the system containing three identical metals. The Yamaguchi correction was not applied in these calculations. Geometry optimizations were carried out using default tolerances of 3×10^{-4} hartree/bohr for the maximum gradient and 5×10^{-6} hartree for the self-consistent field (SCF) energy change between steps. The approximate transition state (TS) structure and barrier heights for the oxo formation step were modeled with the climbing image nudged elastic band (CI-NEB) method.[23] The initial and final states were frozen from prior geometry optimizations and contain M–O and O–N bond lengths, respectively, of 2.52 Å and 1.19 Å for the N_2O adduct and 1.62 Å and 2.98 Å for the Mn(IV)–oxo species. We mapped the reaction coordinate between these states with CI-NEB using a total of 10 images.

The adsorption energy of η^1-N ($\Delta E_{ads}(\eta^1\text{-N})$) and η^1-O ($\Delta E_{ads}(\eta^1\text{-O})$) coordinated N_2O in the trimetallic and Mg-diluted M_2(dobdc) clusters was evaluated as follows:

$$\Delta E_{ads}(\eta^1\text{-N}) = E(\text{M-N}_2\text{O}) - E(\text{M}) - E(\text{N}_2\text{O}) \qquad \text{eq. S3}$$

$$\Delta E_{ads}(\eta^1\text{-O}) = E(\text{M-ON}_2) - E(\text{M}) - E(\text{N}_2\text{O}) \qquad \text{eq. S4}$$

where E(M–N_2O) is the energy of the trimetallic or Mg-diluted M_2(dobdc) cluster model with η^1-N coordinated N_2O, E(M–ON_2) is the energy of the cluster with η^1-O coordinated N_2O, E(M) is the energy of the bare cluster, and E(N_2O) is the energy of an N_2O molecule in the gas phase.

Table S11. DFT-calculated energies of adsorption (ΔE_{ads}) of η^1-N and η^1-O coordinated N_2O bound to the open metal site of the trimetallic and Mg-diluted M_2(dobdc) cluster models.

	Energy of adsorption (kJ/mol)			
	Trimetallic		Mg-diluted	
Metal	**η^1-N**	**η^1-O**	**η^1-N**	**η^1-O**
Mg	−53.4	−64.5	-	-
Mn	−69.7	−68.4	−43.9	−48.8
Fe	−53.2	−53.7	−50.0	−54.8
Co	−53.4	−57.7	−53.7	−58.3
Ni	−56.9	−62.2	−54.4	−64.1
Cu	−41.7	−46.1	−47.2	−46.7
Zn	−49.0	−51.9	−50.4	−53.7

Table S12. Bond angles and bond lengths of N_2O bound to the open metal site of the trimetallic and Mg-diluted M_2(dobdc) cluster models in η^1-N and η^1-O coordination modes.

	η^1-N		η^1-O	
Cluster	**∠M–N_2O (°)**	**M–N (Å)**	**∠M–ON_2 (°)**	**M–O (Å)**
Mg_3	147.6	2.33	119.7	2.27
Mn_3	172.1	1.95	119.5	2.29
$MnMg_2$	115.7	2.52	107.3	2.52
Co_3	122.4	2.41	118.3	2.38
$CoMg_2$	123.5	2.39	118.0	2.37
Fe_3	122.6	2.41	109.5	2.41
$FeMg_2$	121.5	2.47	109.1	2.43
Ni_3	122.2	2.42	117.8	2.34
$NiMg_2$	132.0	2.25	118.7	2.29
Cu_3	108.3	2.57	105.8	2.52
$CuMg_2$	115.3	2.57	105.3	2.54
Zn_3	118.2	2.55	108.2	2.45
$ZnMg_2$	118.9	2.52	108.9	2.44

Table S13. Spin multiplicity (i.e., $2S+1$) of the trimetallic and Mg-diluted M_2(dobdc) cluster models.

	Spin multiplicity	
Metal	**Trimetallic**	**Mg-diluted**
Mg	1	-
Mn	10	4
Fe	13	5
Co	10	4
Ni	7	3
Cu	4	2
Zn	1	1

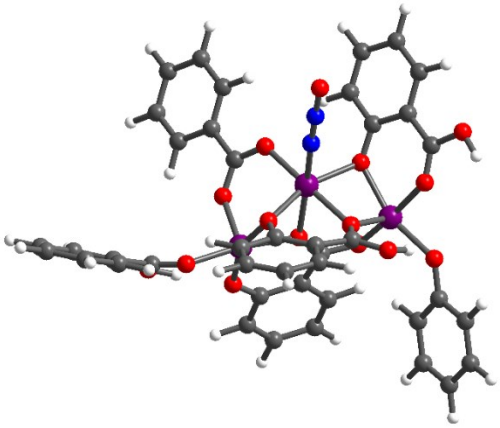

Figure S68. DFT-calculated structure of η^1-N coordinated N_2O in the trimetallic Mn-based cluster model. Bond lengths: Mn–N (1.95 Å), N–N (1.13 Å), N–O (1.18 Å). ∠M–N_2O = 172.1 °. Purple, blue, gray, red and white spheres represent manganese, nitrogen, carbon, oxygen, and hydrogen atoms, respectively.

The adsorption energy of η^1-N ($\Delta E_{ads}(\eta^1\text{-N})$) and η^1-O ($\Delta E_{ads}(\eta^1\text{-O})$) coordinated N_2O in the center or edge metal spin-flipped trimetallic clusters was evaluated using the same procedure as in the previous system. However, the spin orientation of electrons in open shell metals were flipped, as illustrated in Figure S69. Spin densities were visually inspected to ensure the BS-DFT calculations converged to the desired states, and the results of the trimetallic Mn_2(dobdc) cluster model are represented in Figure S70.

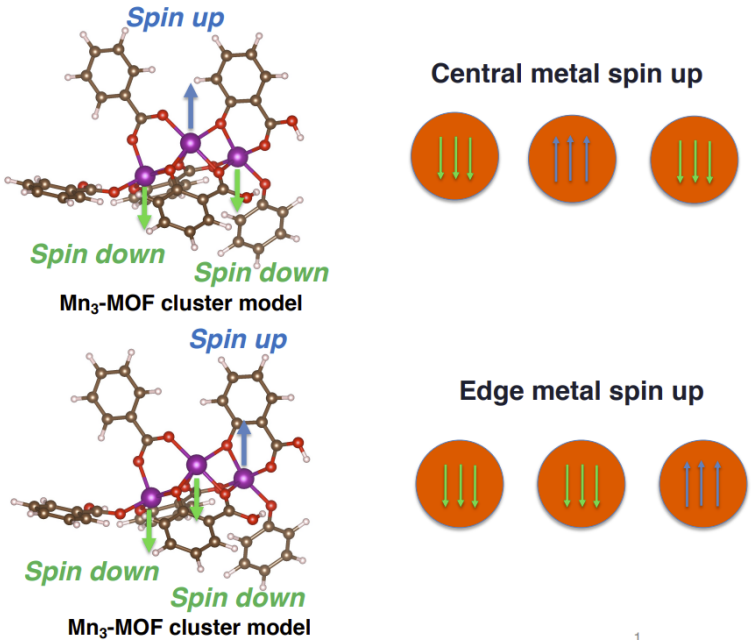

Figure S69. Structures of the central and edge metal spin-flipped configurations of the trimetallic Mn_2(dobdc) cluster and the corresponding high spin electron configuration of the systems. Purple, brown, red, and white spheres represent manganese, carbon, oxygen, and hydrogen atoms, respectively.

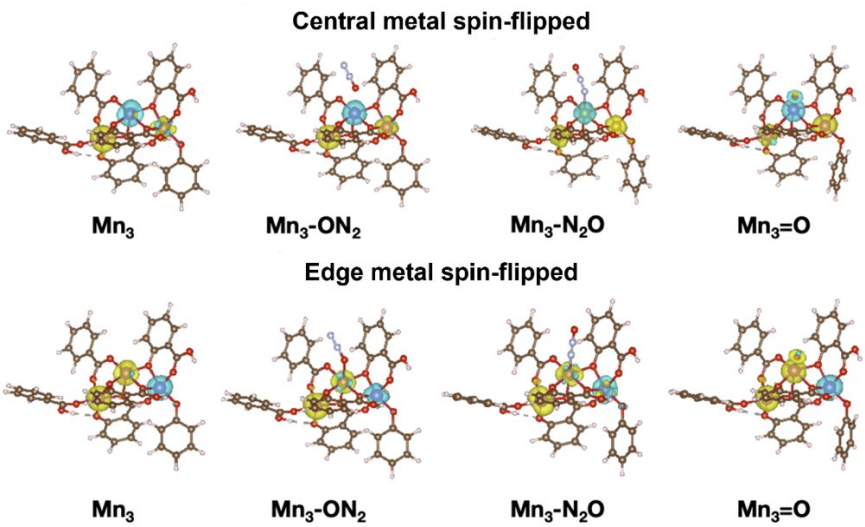

Figure S70. Spin densities of the central and edge metal spin-flipped Mn trimetallic cluster models and various intermediates. Yellow and light blue isosurfaces represent positive and negative spin densities, respectively. An isosurface value of 0.01 e/bohr^3 is used for all visualizations. Orange, brown, red, and white spheres represent manganese, carbon, oxygen, and hydrogen atoms, respectively.

Table S14. Broken symmetry DFT-calculated energies of adsorption (ΔE_{ads}) of η^1-N and η^1-O coordinated N_2O bound to the open metal site of the open shell trimetallic M_2(dobdc) cluster models in central or edge metal spin-flipped configurations.

	Energy of adsorption (kJ/mol)			
	Central Metal		**Edge Metal**	
Metal	**η^1-N**	**η^1-O**	**η^1-N**	**η^1-O**
Mn	119.3	−252.2	299.9	116.3
Fe	−290.7	−291.2	−53.1	−53.6
Co	−251.2	−255.5	−53.3	−57.7
Ni	−56.8	−62.1	−56.7	−57.1
Cu	−46.9	−46.1	−44.8	−46.1

The energies of M(IV)–oxo formation ($\Delta E_f(M^{(n+2)}\text{-oxo})$) in the trimetallic and Mg-diluted M_2(dobdc) cluster models was evaluated as follows:

$$\Delta E_f\left(M^{(n+2)}\text{–oxo}\right) = E\left(M^{(n+2)}\text{–oxo}\right) + E(N_2) - E(M^n) - E(N_2O) \qquad \text{eq. S5}$$

where $E(M^{(n+2)}\text{–oxo})$ is the energy of the oxo-containing trimetallic or Mg-diluted M_2(dobdc) cluster, $E(M^n)$ is the energy of the bare cluster, $E(N_2)$ is the energy of an N_2 molecule in the gas phase, and $E(N_2O)$ is the energy of an N_2O molecule in the gas phase.

Table S15. DFT-calculated energies of M(IV)–oxo formation (ΔE_f(M–oxo)) in the trimetallic and Mg-diluted M_2(dobdc) cluster models.

	M(IV)-oxo formation (kJ/mol)	
Metal	**Trimetallic**	**Mg-diluted**
Mg	96.7	96.7
Mn	−183.1	−176.1
Fe	−55.5	−52.7
Co	28.5	9.9
Ni	104.2	73.0
Cu	104.6	64.9
Zn	96.8	89.6

Table S16. DFT-calculated M–O bond lengths in M(IV)–oxo (Å) trimetallic and Mg-diluted M_2(dobdc) cluster models.

	M(IV)–oxo bond length (Å)	
Metal	**Trimetallic**	**Mg-diluted**
Mg	1.93	1.93
Mn	1.62	1.62
Co	1.63	1.67
Fe	1.61	1.60
Ni	2.41	1.84
Cu	1.82	1.82
Zn	1.89	1.90

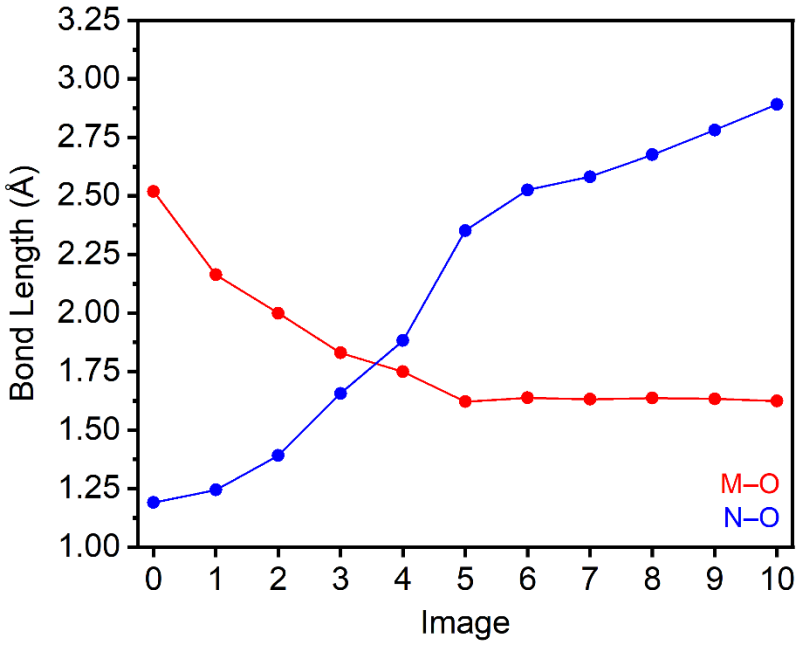

Figure S71. Image number vs. bond length of M–O (red) and N–O (blue) bonds in the CI-NEB calculated reaction coordinate for the activation of N_2O in the Mg-diluted Mn_2(dobdc) model.

15. High-temperature N_2O studies in $Mn_2(dobdc)$

Bulk high-temperature N_2O dosing procedure: $Mn_2(dobdc)$ (107 mg) was dosed with N_2O at 300 °C gradually by performing an N_2O gas sorption measurement at that temperature, starting at very low pressure (<10 mbar) and increasing incrementally up to 1000 mbar then gradually returning to <10 mbar over approximately 26 h. The temperature was maintained throughout the measurement using a sand bath with an internal thermometer. The sample was activated at 300 °C for 24 h under high vacuum (<10 μbar) prior to N_2O dosing.

Variable-temperature DRIFTS analysis: $Mn_2(dobdc)$ was prepared for DRIFTS analysis by mixing it with KBr in an N_2-filled glovebox (~1:2 MOF:KBr by volume), then quickly transferring the mixture to the sample chamber outside of the box. The chamber was immediately sealed and activated for 24 h at 180 °C under high vacuum (<50 mTorr). After activation, the sample chamber was allowed to cool to room temperature and then backfilled with N_2O. The spectrum of activated $Mn_2(dobdc)$ mixed with KBr under N_2O was collected at 25 °C and subtracted from subsequent spectra collected on the identical sample to emphasize any new stretching frequencies attributed to Mn-oxo formation. The sample chamber was then heated to 300 °C under static N_2O and held at that temperature for 15 h. Spectra were collected periodically throughout the duration of the measurement.

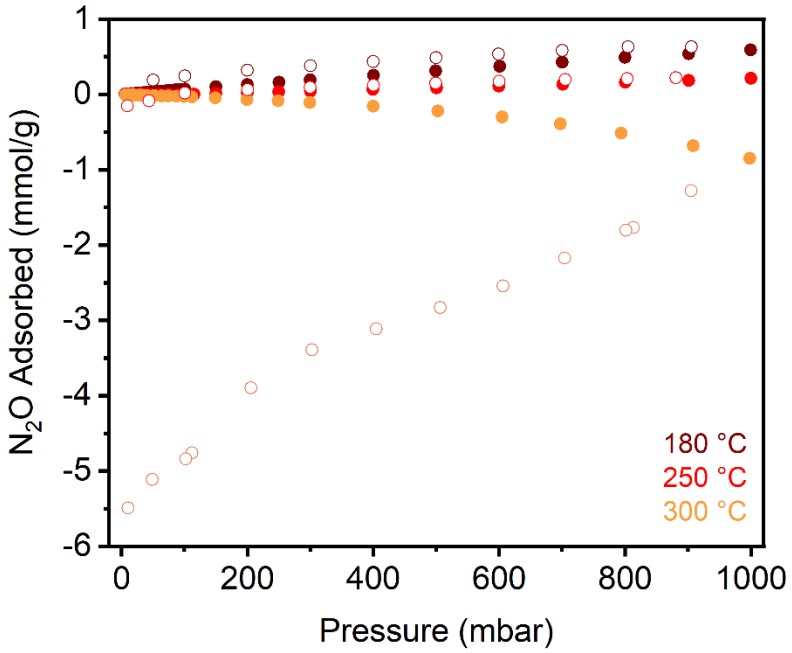

Figure S72. N_2O adsorption (solid circles) and desorption (open circles) isotherms of activated $Mn_2(dobdc)$ at 180 °C (dark red), 250 °C (red), and 300 °C (orange). The sample was reactivated at the temperature of its subsequent adsorption measurement for 24 h under high vacuum (<10 μbar) between isotherms. A data point was considered equilibrated when less than 0.01% change in pressure occurred over a 30 or 60 s interval.

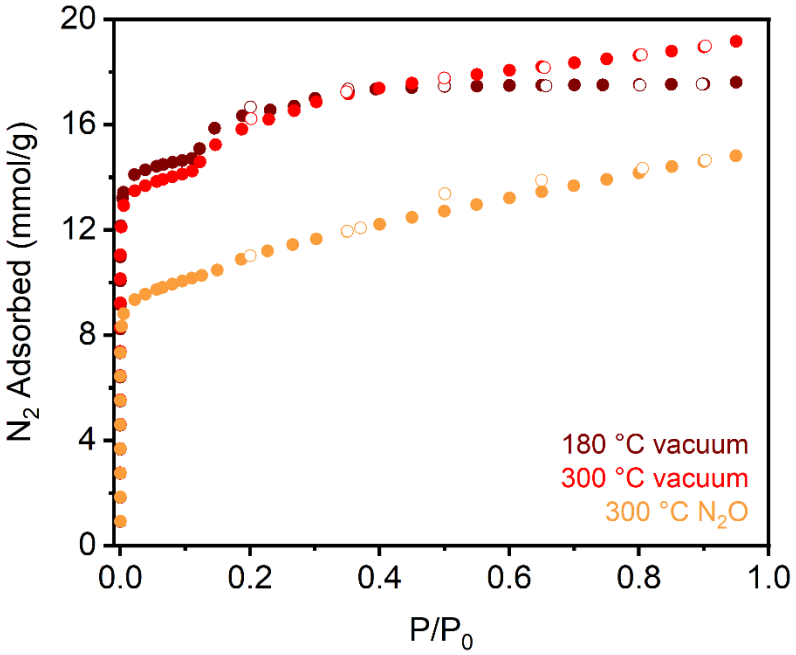

Figure S73. N_2 adsorption (solid circles) and desorption (open circles) isotherms of activated Mn_2(dobdc) at 77 K measured after activation for 24 h at 180 °C (dark red) and 300 °C (red), and after N_2O dosing at 300 °C (orange). The Brunauer-Emmett-Teller (BET) surface areas were determined to be 1344 ± 3 m^2/g after 180 °C activation, 1285 ± 3 m^2/g after 300 °C activation, and 896 ± 2 m^2/g after N_2O dosing at 300 °C.

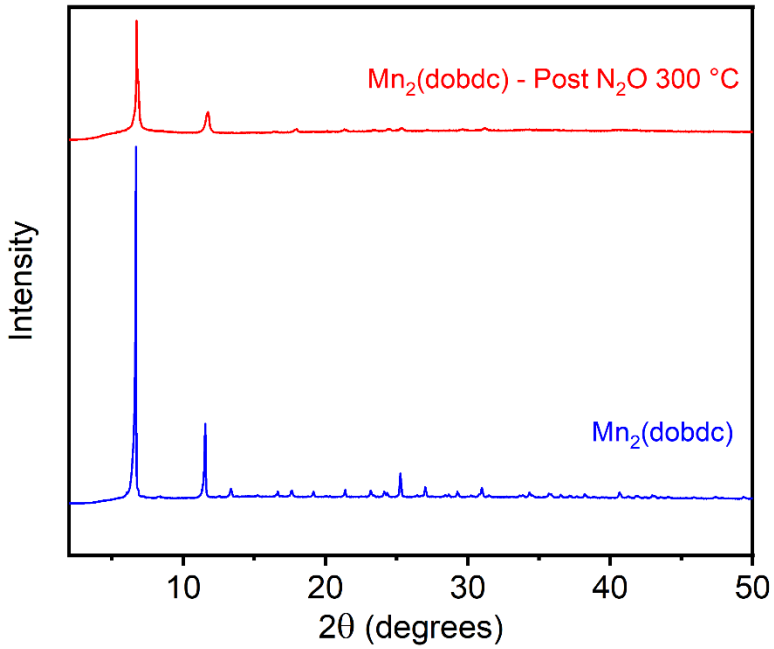

Figure S74. PXRD (λ = 1.54 Å) pattern of activated Mn_2(dobdc) after N_2O dosing at 300 °C. The experimental pattern prior to N_2O dosing is included for reference.

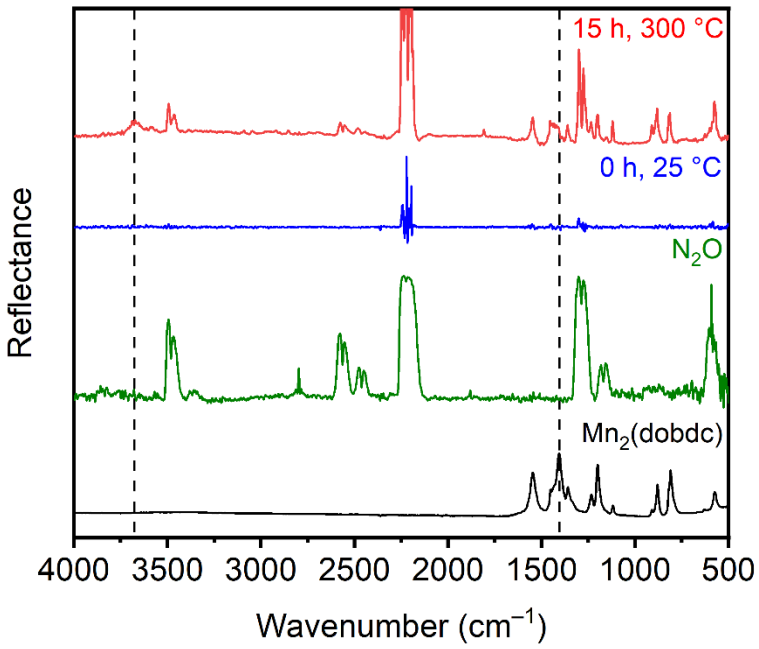

Figure S75. Variable-temperature DRIFTS spectra collected under an atmosphere of N_2O (approx. 1 bar) at 25 °C after 0 h (blue) and 300 °C (red) after 15 h. The DRIFTS spectrum of free N_2O (green) and the ATR-IR spectrum of Mn_2(dobdc) (black) are included for reference. Dotted lines denote changes in the spectrum after N_2O treatment.

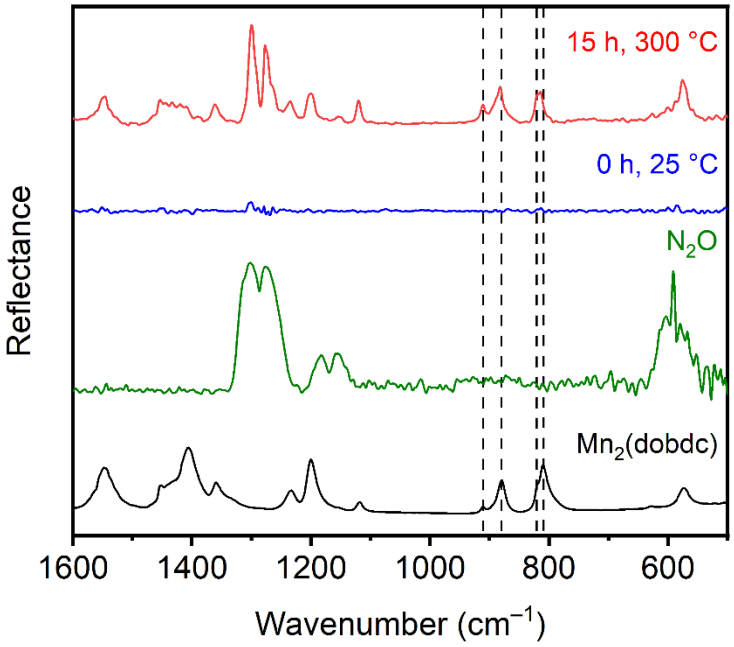

Figure S76. Magnified variable-temperature DRIFTS spectra collected under an atmosphere of N_2O (approx. 1 bar) at 25 °C after 0 h (blue) and 300 °C (red) after 15 h, showing no new stretching frequencies in the region expected for Mn(IV)-oxo formation (~845 cm^{-1}).[24] The DRIFTS spectrum of free N_2O (green) and the ATR-IR spectrum of Mn_2(dobdc) (black) are included for reference. Dotted lines marking Mn_2(dobdc) stretching frequencies are included as visual aids. The stretches that appear after heating to 300 °C match those of unreacted Mn_2(dobdc) and free N_2O. Their prevalence despite subtracting the 25 °C N_2O-dosed spectrum of this sample from all measurements is attributed to thermal excitement at elevated temperatures.

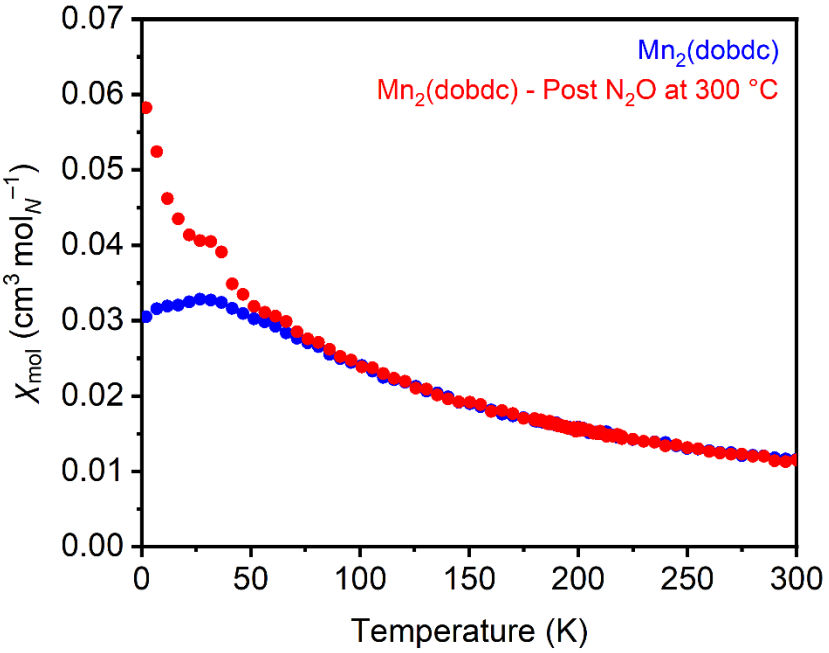

Figure S77. Zero field cooled (ZFC) variable-temperature molar magnetic susceptibility (χ_{mol}) measurements of $Mn_2(dobdc)$ before (blue) and after (red) N_2O dosing at 300 °C under an applied field of 1000 Oe.

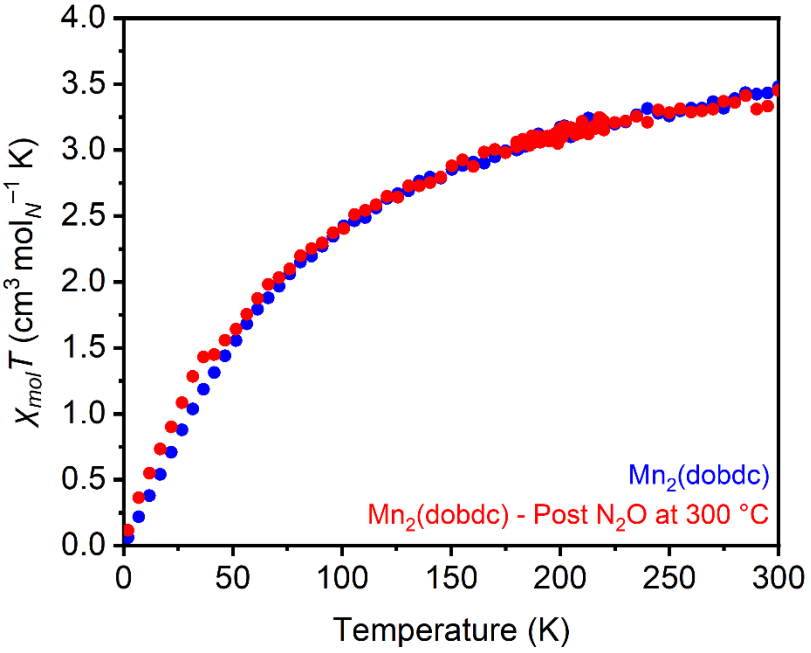

Figure S78. ZFC variable-temperature temperature-adjusted molar magnetic susceptibility ($\chi_{mol}T$) measurements of $Mn_2(dobdc)$ before (blue) and after (red) N_2O dosing at 300 °C under an applied field of 1000 Oe.

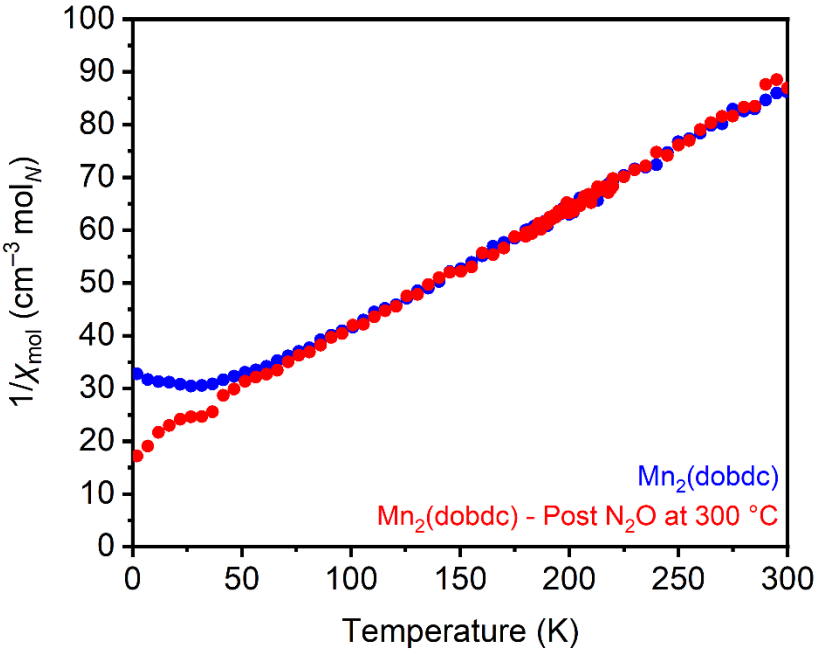

Figure S79. ZFC variable-temperature inverse molar magnetic susceptibility ($1/\chi_{mol}$) measurements of Mn_2(dobdc) before (blue) and after (red) N_2O dosing at 300 °C under an applied field of 1000 Oe.

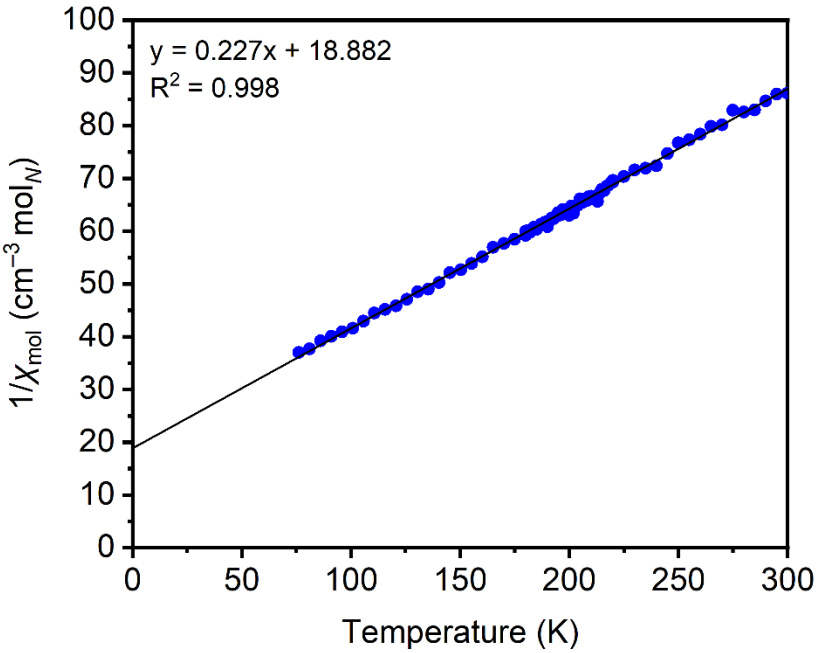

Figure S80. Fit of the inverse molar magnetic susceptibility ($1/\chi_{mol}$) of Mn_2(dobdc) within the region (75–300 K) where the data are linear. The effective magnetic moment (μ_{eff}) of Mn_2(dobdc) calculated from this fit is 5.94 Bohr magnetons (μB) (theoretical μ_{eff} for an S = 5/2 system: 5.92 μB).

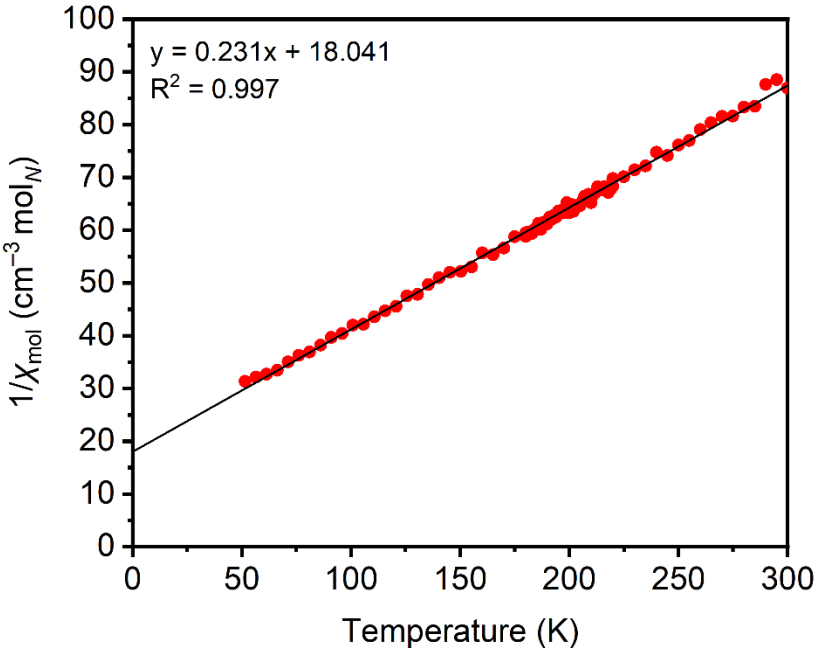

Figure S81. Fit of the inverse molar magnetic susceptibility (1/ χ_{mol}) of Mn_2(dobdc) after N_2O treatment at 300 °C within the region (50–300 K) where the data are linear. The effective magnetic moment (μ_{eff}) of Mn_2(dobdc) calculated from this fit is 5.89 Bohr magnetons (μB) (theoretical μ_{eff} for an S = 5/2 system: 5.92 μB).

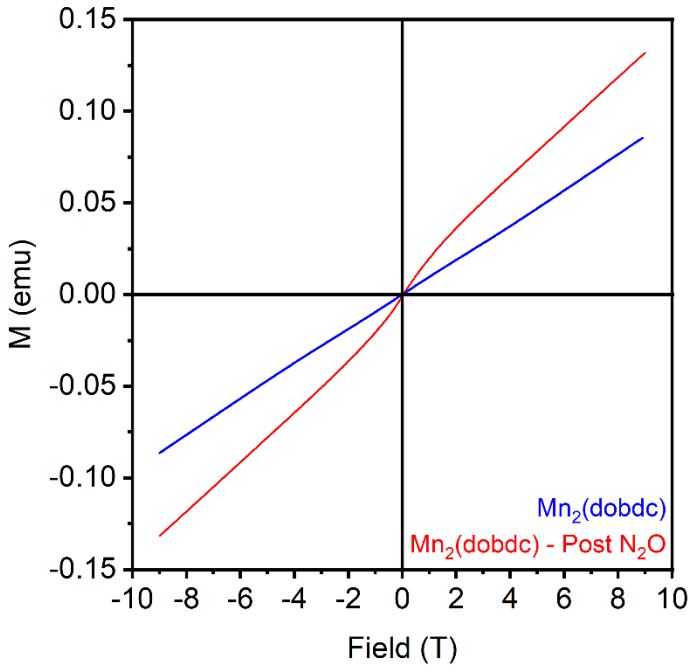

Figure S82. Moment vs field measurements collected at 5 K on Mn_2(dobdc) before (blue) and after (red) treatment with N_2O at 300 °C.

16. References

(1) Dietzel, P. D. C.; Johnsen, R. E.; Blom, R.; Fjellvåg, H. Structural Changes and Coordinatively Unsaturated Metal Atoms on Dehydration of Honeycomb Analogous Microporous Metal–Organic Frameworks. *Chem. Eur. J.* **2008**, *14* (8), 2389–2397. https://doi.org/10.1002/chem.200701370.

(2) Denysenko, D.; Grzywa, M.; Tonigold, M.; Streppel, B.; Krkljus, I.; Hirscher, M.; Mugnaioli, E.; Kolb, U.; Hanss, J.; Volkmer, D. Elucidating Gating Effects for Hydrogen Sorption in MFU-4-Type Triazolate-Based Metal-Organic Frameworks Featuring Different Pore Sizes. *Chem. Eur. J.* **2011**, *17* (6), 1837–1848. https://doi.org/10.1002/chem.201001872.

(3) Chichak, K.; Jacquemard, U.; Branda, N. R. The Construction of (Salophen)Ruthenium(II) Assemblies Using Axial Coordination. *Eur. J. Inorg. Chem.* **2002**, *2002* (2), 357–368. https://doi.org/10.1002/1099-0682(20022)2002:2<357::AID-EJIC357>3.0.CO;2-T.

(4) Rieth, A. J.; Tulchinsky, Y.; Dincă, M. High and Reversible Ammonia Uptake in Mesoporous Azolate Metal–Organic Frameworks with Open Mn, Co, and Ni Sites. *J. Am. Chem. Soc.* **2016**, *138* (30), 9401–9404. https://doi.org/10.1021/jacs.6b05723.

(5) Rieth, A. J.; Wright, A. M.; Skorupskii, G.; Mancuso, J. L.; Hendon, C. H.; Dincă, M. Record-Setting Sorbents for Reversible Water Uptake by Systematic Anion Exchanges in Metal–Organic Frameworks. *J. Am. Chem. Soc.* **2019**, *141* (35), 13858–13866. https://doi.org/10.1021/jacs.9b06246.

(6) Park, S. S.; Tulchinsky, Y.; Dincă, M. Single-Ion Li^+, Na^+, and Mg^{2+} Solid Electrolytes Supported by a Mesoporous Anionic Cu–Azolate Metal–Organic Framework. *J. Am. Chem. Soc.* **2017**, *139* (38), 13260–13263. https://doi.org/10.1021/jacs.7b06197.

(7) Zick, M. E.; Lee, J.-H.; Gonzalez, M. I.; Velasquez, E. O.; Uliana, A. A.; Kim, J.; Long, J. R.; Milner, P. J. Fluoroarene Separations in Metal–Organic Frameworks with Two Proximal Mg^{2+} Coordination Sites. *J. Am. Chem. Soc.* **2021**, *143* (4), 1948–1958. https://doi.org/10.1021/jacs.0c11530.

(8) Queen, W. L.; Hudson, M. R.; Bloch, E. D.; Mason, J. A.; Gonzalez, M. I.; Lee, J. S.; Gygi, D.; Howe, J. D.; Lee, K.; Darwish, T. A.; James, M.; Peterson, V. K.; Teat, S. J.; Smit, B.; Neaton, J. B.; Long, J. R.; Brown, C. M. Comprehensive Study of Carbon Dioxide Adsorption in the Metal–Organic Frameworks M_2(dobdc) (M = Mg, Mn, Fe, Co, Ni, Cu, Zn). *Chem. Sci.* **2014**, *5* (12), 4569–4581. https://doi.org/10.1039/C4SC02064B.

(9) Zhou, W.; Wu, H.; Yildirim, T. Enhanced H_2 Adsorption in Isostructural Metal−Organic Frameworks with Open Metal Sites: Strong Dependence of the Binding Strength on Metal Ions. *J. Am. Chem. Soc.* **2008**, *130* (46), 15268–15269. https://doi.org/10.1021/ja807023q.

(10) Geier, S. J.; Mason, J. A.; Bloch, E. D.; Queen, W. L.; Hudson, M. R.; Brown, C. M.; Long, J. R. Selective Adsorption of Ethylene over Ethane and Propylene over Propane in the Metal–Organic Frameworks M_2(dobdc) (M = Mg, Mn, Fe, Co, Ni, Zn). *Chem. Sci.* **2013**, *4* (5), 2054–2061. https://doi.org/10.1039/c3sc00032j.

(11) Bloch, E. D.; Murray, L. J.; Queen, W. L.; Chavan, S.; Maximoff, S. N.; Bigi, J. P.; Krishna, R.; Peterson, V. K.; Grandjean, F.; Long, G. J.; Smit, B.; Bordiga, S.; Brown, C. M.; Long, J. R. Selective Binding of O_2 over N_2 in a Redox–Active Metal–Organic Framework with Open Iron(II) Coordination Sites. *J. Am. Chem. Soc.* **2011**, *133* (37), 14814–14822. https://doi.org/10.1021/ja205976v.

(12) Xiao, D. J.; Bloch, E. D.; Mason, J. A.; Queen, W. L.; Hudson, M. R.; Planas, N.; Borycz, J.; Dzubak, A. L.; Verma, P.; Lee, K.; Bonino, F.; Crocellà, V.; Yano, J.; Bordiga, S.; Truhlar,

D. G.; Gagliardi, L.; Brown, C. M.; Long, J. R. Oxidation of Ethane to Ethanol by N_2O in a Metal–Organic Framework with Coordinatively Unsaturated Iron(II) Sites. *Nat. Chem.* **2014**, *6* (7), 590–595. https://doi.org/10.1038/nchem.1956.

(13) Gonzalez, M. I.; Kapelewski, M. T.; Bloch, E. D.; Milner, P. J.; Reed, D. A.; Hudson, M. R.; Mason, J. A.; Barin, G.; Brown, C. M.; Long, J. R. Separation of Xylene Isomers through Multiple Metal Site Interactions in Metal–Organic Frameworks. *J. Am. Chem. Soc.* **2018**, *140* (9), 3412–3422. https://doi.org/10.1021/jacs.7b13825.

(14) Mason, J. A.; Veenstra, M.; Long, J. R. Evaluating Metal–Organic Frameworks for Natural Gas Storage. *Chem. Sci.* **2014**, *5* (1), 32–51. https://doi.org/10.1039/C3SC52633J.

(15) Neese, F. The ORCA Program System. *WIREs Comput Mol Sci* **2012**, *2* (1), 73–78. https://doi.org/10.1002/wcms.81.

(16) Becke, A. D. Density-Functional Thermochemistry. III. The Role of Exact Exchange. *J. Chem. Phys.* **1993**, *98* (7), 5648–5652. https://doi.org/10.1063/1.464913.

(17) Grimme, S.; Antony, J.; Ehrlich, S.; Krieg, H. A Consistent and Accurate *Ab Initio* Parametrization of Density Functional Dispersion Correction (DFT-D) for the 94 Elements H-Pu. *J. Chem. Phys.* **2010**, *132* (15), 154104. https://doi.org/10.1063/1.3382344.

(18) Grimme, S.; Ehrlich, S.; Goerigk, L. Effect of the Damping Function in Dispersion Corrected Density Functional Theory. *J. Comput. Chem.* **2011**, *32* (7), 1456–1465. https://doi.org/10.1002/jcc.21759.

(19) Van Lenthe, E.; Ehlers, A.; Baerends, E.-J. Geometry Optimizations in the Zero Order Regular Approximation for Relativistic Effects. *J. Chem. Phys.* **1999**, *110* (18), 8943–8953. https://doi.org/10.1063/1.478813.

(20) Weigend, F.; Ahlrichs, R. Balanced Basis Sets of Split Valence, Triple Zeta Valence and Quadruple Zeta Valence Quality for H to Rn: Design and Assessment of Accuracy. *Phys. Chem. Chem. Phys.* **2005**, *7* (18), 3297. https://doi.org/10.1039/b508541a.

(21) Neese, F.; Wennmohs, F.; Hansen, A.; Becker, U. Efficient, Approximate and Parallel Hartree–Fock and Hybrid DFT Calculations. A 'Chain-of-Spheres' Algorithm for the Hartree–Fock Exchange. *Chemical Physics* **2009**, *356* (1–3), 98–109. https://doi.org/10.1016/j.chemphys.2008.10.036.

(22) Neese, F. Definition of Corresponding Orbitals and the Diradical Character in Broken Symmetry DFT Calculations on Spin Coupled Systems. *Journal of Physics and Chemistry of Solids* **2004**, *65* (4), 781–785. https://doi.org/10.1016/j.jpcs.2003.11.015.

(23) Henkelman, G.; Uberuaga, B. P.; Jónsson, H. A Climbing Image Nudged Elastic Band Method for Finding Saddle Points and Minimum Energy Paths. *J. Chem. Phys.* **2000**, *113* (22), 9901–9904. https://doi.org/10.1063/1.1329672.

(24) Halbach, R. L.; Gygi, D.; Bloch, E. D.; Anderson, B. L.; Nocera, D. G. Structurally Characterized Terminal Manganese(IV) Oxo Tris(Alkoxide) Complex. *Chem. Sci.* **2018**, *9* (19), 4524–4528. https://doi.org/10.1039/C8SC01164H.